Mälardalen University
Division of Mathematics and Physics
Västerås, Sweden

Thesis for the Degree of Master of Science in Mathematics/Applied Mathematics with Specialization in Financial Engineering. 30.0 credits

PARAMETER STABILITY IN ADDITIVE NORMAL TEMPERED STABLE PROCESSES FOR EQUITY DERIVATIVES

Eduardo Alberto Alcántara Martínez
eduardo_alcantara10@outlook.com

Examiner: Achref Bachouch
Mälardalen University, Västerås, Sweden

Supervisor(s): Jan Röman, Ying Ni
Mälardalen University, Västerås, Sweden

05/06/2023

Abstract

This thesis focuses on the parameter stability of additive normal tempered stable processes when calibrating a volatility surface. The studied processes arise as a generalization of Lévy normal tempered stable processes, and their main characteristic are their time-dependent parameters. The theoretical background of the subject is presented, where its construction is discussed taking as a starting point the definition of Lévy processes. The implementation of an option valuation model using Fourier techniques and the calibration process of the model are described. The thesis analyzes the parameter stability of the model when it calibrates the volatility surface of a market index (EURO STOXX 50) during three time spans. The time spans consist of the periods from Dec 2016 to Dec 2017 (after the Brexit and the US presidential elections), from Nov 2019 to Nov 2020 (during the pandemic caused by COVID-19) and a more recent time period, April 2023. The findings contribute to the understanding of the model itself and the behavior of the parameters under particular economic conditions.

Keywords: *Parameter Stability, Lévy Processes, Calibration, Volatility Surface, Subordination, Additive Normal Tempered Stable Processes, Stable Distribution, Variance Gamma Process, Normal Inverse Gaussian Process.*

Acknowledgements

I would like to express my sincere thanks to my parents for their constant support during my academic and professional journey. Their encouragement, understanding, and sacrifice have been crucial in helping me achieve my goals. I would also like to extend my gratitude to my sister, who has been a constant source of inspiration and guidance in my life.

Contents

List of Figures

List of Tables

List of Acronyms

ATS Additive Normal Tempered Stable Processes

LTS Normal Tempered Stable Processes

NIG Normal Inverse Gaussian

IG Inverse Gaussian

VG Variance Gamma

FT Fourier Transform

FFT Fast Fourier Transform

Chapter 1

Introduction

The study of financial markets and asset pricing has long been an intriguing field of research due to its complex and dynamic nature. Over the years, various mathematical models and techniques have been developed to capture the underlying dynamics of asset prices. The Black-Scholes model is probably the most widely recognized and utilized option pricing model in finance.

However, it has been shown that the Black-Scholes model has some drawbacks of significant importance while modeling equity derivatives. One of those problems is that the presence of a volatility smile suggests that in the risk neutral world, the kurtosis should be higher than the one provided while using normal densities. Another problem is that the distribution of the returns does not tend to be symmetric, instead one could expect a distribution with a left tail fatter than the right one, this can be measured with the skewness. To overcome these problems, particular classes of stochastic processes have been studied in the recent years.

Lévy processes are one of those examples. They are defined as right-continuous stochastic processes with left limits that satisfy three properties: independent increments, stationary increments and stochastic continuity. One particular extension of Lévy processes are the Normal Tempered Stable Processes (LTS), which were first introduced in [1] where a particular case of LTS processes was studied: The Variance Gamma (VG) process. LTS processes possess properties that provide a flexible framework for modeling financial data due to their ability to capture both heavy-tailed and asymmetric behavior. The study of LTS processes continued in [2] where the VG process was generalized and in [3], where the Normal Inverse Gaussian (NIG) process was studied.

Even if LTS processes incorporate realistic properties while modeling financial instruments, the assumption of stationary increments for model calibration has been studied and discussed in [4], where it was shown that even if LTS processes calibrate the implied volatility in a satisfactory way for a single maturity, they fail to reproduce the volatility surface when many maturities are considered.

Additionally, the stationary increments in LTS processes impose some restrictions that lead to rigid scaling properties, something that is not observed when returns series are analyzed empirically. Another argument that questions the stationary assumption is given in [5], where it is mentioned that a market maker does not consider the consequences of a jump to be equivalent for options of different maturities. With a hedging perspective, the important factor after a jump arrival is the amount of trading required over the underlying to replicate the option, making the impact of the jump and the maturity of the option inhomogeneous.

To overcome the previous inconveniences, time inhomogeneous jump processes were proposed. The probability characterization of these processes can be found in [6], while some of the initial applications in option pricing were developed in [7] and [8].

More recently, a particular class of additive processes were defined and studied in [5], which the authors called ATS. ATS processes show a significant improvement when calibrating volatility surfaces for equity derivatives. These type of processes have independent increments and stochastic continuity but they do not have stationary increments. One of the main changes compared to LTS processes is that ATS processes have deterministic and time-dependent parameters, and given a fixed time t, a LTS process can be associated, allowing to preserve properties of these processes.

The objective of this thesis is to analyze the behavior of the parameters of the ATS processes over different time periods when calibrating the volatility surface of a market index (EURO STOXX 50) using an option pricing model that incorporates these processes. Additionally, the calibration performance using ATS models will be compared with its corresponding LTS process. It builds upon the analysis done in [5], which looked at specific dates. This thesis aims to gain a better understanding of how these parameters change under different economic conditions.

The analyzed option data consists of a data set containing observations of daily option prices of European call options with the EURO STOXX 50 index as underlying. The first time period corresponds from January 2017 to December 2017. The second time period corresponds from November 2019 to November 2020 and the last time period contemplates information from March 31^{st} to April 28^{th}, 2023.

The experimental results show that the ATS processes significantly outperform their corresponding LTS processes in every time period. Besides, when the market volatilities present a steep slope in the short term maturities (a situation that is more likely in stress periods such as in March 2020) the calibration of LTS processes failed while the calibration for ATS processes show a significant increment in one of the parameters, and as a consequence of this increment the average volatility of the surface decreases without reflecting the real market conditions.

The distribution of the thesis is as follows: in Chapter 2 the construction and properties of LTS processes is explained using as main references [4] and [6]. The most relevant examples of LTS processes, the NIG process and the VG, are discussed. Subsequently, the results that allow the extension from LTS processes to ATS processes are presented and explained following [5].

Once the theoretical background is set, in Chapter 3 the model for option pricing that involves ATS processes is described providing a comprehensive understanding of its key components. Section 2 explores the option valuation technique employed in the model, specifically highlighting the use of the Fast Fourier Transform (FFT) for efficient calculations. The chapter finishes discussing the calibration process and the optimization method that will be employed.

Finally, Chapter 4 will provide a detailed explanation of the market data used for the analysis, as well as the calibration procedure and the main results will be presented. Chapter 5 concludes.

Remark: The code utilized in this thesis has been stored in a GitHub repository for convenient access and reference. The repository can be found at the following link: https://github.com/EduardoAlca10/Master-ATS-work-code. Interested individuals can visit the repository to examine the code in detail, facilitating a deeper understanding of the technical aspects discussed in this thesis.

Chapter 2

Theoretical Background

This chapter aims to provide a solid understanding of the theoretical framework behind ATS processes, which will be crucial for their successful application in the calibration of implied volatilities. Since ATS processes are a generalization of LTS processes, Sections 1, 2 and 3 will be useful to understand every element in the construction of LTS processes. In particular, it will be introduced the concepts of Lévy processes, stable processes and tempered stable distributions, which are a generalization of stable distributions that incorporate exponential damping.

In Section 4, LTS processes will be defined by explaining the Brownian subordination technique, and the two main examples of these processes, the VG nd the NIG process, will be presented. Finally, in Section 5, ATS processes will be defined as a particular subclass of additive processes.

1 Lévy Processes

The purpose of this section is to state the Lévy-Itô decomposition theorem following [4], and explain in an intuitive way which elements fully characterizes a Lévy process. To do that, it will be given the necessary definitions and intuitive ideas to understand the theorem since it is of relevance importance for subsequent sections.

Definition 2.1: ***Lévy Process [4]:*** *A cadlag stochastic process* [1] $(X_t)_{t\geq 0}$ *on* $(\Omega, \mathcal{F}, \mathbb{P})$ *with values in* $\mathbb{R}^d$ *such that* $X_0 = 0$ *is called a Lévy process if it possesses the following properties:*

1. *Independent increments: for every increasing sequence of times* $t_0, ..., t_n$*, the random variables* $X_{t_0}, X_{t_1} - X_{t_0}, ..., X_{t_n} - X_{t_{n-1}}$ *are independent.*
2. *Stationary increments: the law* [2] *of* $X_{t+h} - X_t$ *does not depend on* t*.*
3. *Stochastic continuity:* $\forall \epsilon > 0$, $\lim_{h\to 0} P(|X_{t+h} - X_t| \geq \epsilon) = 0$.

The condition $X_0 = 0$, with independent and stationary increments, is something that we observe in the definition of the Brownian motion. However, a Lévy process is more general since the increments do not need to be normally distributed, and the paths do not need to be continuous. The interpretation of the third condition implies that the jumps that generate discontinuities are indeed random, given that the probability to see a jump at time t is zero.

In general, the Lévy-Itô decomposition theorem says that each Lévy process is characterized by the so called characteristic triplet (A, υ, γ). However, to understand each element in the triplet, and to eventually state the Lévy-Itô decomposition theorem, it is necessary to give some definitions and concepts that can be divided in three groups:

- First Group: Radon, Poisson and Lévy measures.

[1] This means that $(X_t)_{t\geq 0}$ is right-continuous with left limits.
[2] We can understand the law of a random variable as its distribution.

- Second Group: Jump measure of a compound Poisson process.
- Third Group: Lévy processes in terms of Brownian and jump processes.

First Group:

Definition 2.2: ***Radon Measure [4]:*** *Let $E \in \mathbb{R}^d$. A Radon measure on $(E, \mathcal{B})$[3] is a measure μ such that for every closed, bounded and measurable set $B \in \mathcal{B}$, $\mu(B) < \infty$.*

Definition 2.3: ***Poisson random Measure [4]:*** *Let $(\Omega, \mathcal{F}, \mathbb{P})$ be a probability space, $E \subset \mathbb{R}^d$ and μ a given positive Radon measure μ on $(E, \mathcal{E})$. A Poisson random measure on E with intensity measure μ is an integer valued random measure:*

$$\begin{aligned} M: \quad & \Omega \times \mathcal{E} \to \mathbb{N} \\ & (\omega, A) \rightarrowtail M(\omega, A), \end{aligned}$$

such that,

1. *For (almost all) $\omega \in \Omega$, $M(\omega, .)$ is an integer-valued Radon measure on E: for any bounded measurable $A \subset E, M(A) < \infty$ is an integer valued random variable.*
2. *For each measurable set $A \subset E, M(., A) = M(A)$ is a Poisson random variable with parameter $\mu(A)$:*
$$\forall k \in \mathbb{N}, \qquad \mathbb{P}(M(A) = k) = e^{-\mu(A)} \frac{(\mu(A)^k)}{k!}.$$
3. *For disjoint measurable sets $A_1, ..., A_n \in E$, the variables $M(A_1), ..., M(A_n)$ are independent.*

To every cadlag process and in particular to every compound Poisson process[4] $(X_t)_t \geq 0$ on $\mathbb{R}^d$ one can associate a random measure on $\mathbb{R}^d \times [0, \infty)$ describing the jumps of X: for any measurable set $B \subset \mathbb{R}^d \times [0, \infty)$

$$J_X(B) = \#(t, X_t - X_{t-}) \in B.$$

For every measurable set $A \subset \mathbb{R}^d$, $J_X([t_1, t_2] \times A)$ counts the number of jump times of X between t_1 and t_2 such that their jump sizes are in A.

Definition 2.4: ***Lévy Measure [4]:*** *Let $(X_t)_{t \geq 0}$ a Lévy process on $\mathbb{R}^d$. The measure υ on $\mathbb{R}^d$ defined by*

$$\upsilon(A) = \mathbb{E}[\#\{t \in [0, 1] : \Delta X_t \neq 0, \Delta X_t \in A\}], \qquad A \in \mathcal{B}(\mathbb{R}^d)$$

is called the Lévy measure of X: $\upsilon(A)$ is the expected number, per unit time, of jumps whose size belongs to A.

Second Group:

Proposition 2.5: ***Jump measure of a compound Poisson process [4]:*** *Let $(X_t)_{t \geq 0}$ be a compound Poisson process with intensity λ and jump size distribution f. Its jump measure J_X is a Poisson random measure on $\mathbb{R}^d \times [0, \infty)$ with intensity measure $\mu(dx \times dt) = \upsilon(dx)dt = \lambda f(dx)dt$.*

This implies that every compound Poisson process can be represented in the following form:

$$X_t = \sum_{s \in [0,t]} \Delta X_s = \int_{[0,t] \times \mathbb{R}^d} x \, J_X(ds \times dx). \tag{2.1}$$

Third Group:

It is possible to consider a Brownian motion with drift $\gamma t + W_t$, and a piece-wise constant Lévy process X_t^0 represented by a compound Poisson process with intensity measure $\upsilon(dx)dt$. The sum

[3] In this case, $\mathcal{B}$ is a σ-algebra of subsets of E.

[4] A compound Poisson process with intensity $\lambda > 0$ and jump size distribution f is a stochastic process X_t defined as $X_t = \sum_{i=1}^{N_t} Y_i$, where jumps sizes Y_i are i.i.d. with distribution f and (N_t) is a Poisson process with intensity λ, independent from $(Y_i)_i \geq 1$.

of these two processes define another Lévy process and it will contain three elements, a drift, a Brownian motion and a jump component.

The Lévy-Itô Decomposition theorem states that, actually, for every Lévy process exists a vector γ, a positive definite matrix A, and a positive measure υ that uniquely determine its distribution. The triplet (A, υ, γ) is called characteristic triplet or Lévy triplet of the process X_t.

Theorem 2.6: ***Lévy-Itô Decomposition [4]:*** *Let $(X_t)_{t\geq 0}$ a Lévy process on $\mathbb{R}^d$ and υ its Lévy measure*

- *υ is a Radon measure on $\mathbb{R}^d \backslash \{0\}$ and verifies:*

$$\int_{|x|\leq 1} |x|^2 \, \upsilon(dx) < \infty \qquad \int_{|x|\geq 1} \upsilon(dx) < \infty.$$

- *The jump measure of X, denoted by J_X, is a Poisson random measure on $[0,\infty] \times \mathbb{R}^d$ with intensity measure $\upsilon(dx)dt$.*

- *There exist a vector γ and a d-dimensional Brownian motion $(B_t)_{t\geq 0}$ with covariance matrix A such that*

$$\begin{aligned} X_t = &\quad \gamma t + B_t + X_t^l + \lim_{\epsilon \downarrow 0} \tilde{X}_t^\epsilon, \qquad \textit{where} \\ X_t^l = &\quad \int_{|x|\geq 1, s\in[0,t]} x \, J_X(ds \times dx) \qquad \textit{and} \\ \tilde{X}_t^\epsilon = &\quad \int_{\epsilon \leq |x| < 1, s\in[0,t]} x \, \{J_X(ds \times dx) - \upsilon(dx)ds\} \\ \equiv &\quad \int_{\epsilon \leq |x| < 1, s\in[0,t]} x \, \tilde{J}_X(ds \times dx). \end{aligned}$$

  The terms in the previous equation are independent and the convergence in the last term is almost sure and uniform in t on $[0,T]$.

In the third point we can observe how X_t is decomposed in four elements. The first two $(\gamma t + B_t)$ represent a continuous Gaussian Lévy process that is uniquely represented by the drift γ and the covariance matrix of Brownian motion, which is denoted by A; The third and fourth elements in the sum represent discontinuous jump processes that are described by its associated Lévy measure, υ.

We can observe how the third and fourth term in the sum are a decomposition of the sum/integral presented in Equation (2.1). X_t^l is a compound Poisson process and represents the elements in the sum which absolutes value of the jumps are larger than 1. The convergence of the sum of these elements is guaranteed by the second condition over the Lévy measure stated in the first point of the theorem, because it ensures that the number of jumps with absolute value larger than 1 is a finite number.

On the other hand, $\tilde{X}_t^\epsilon$ is also a compound Poisson process and represents the sum of the terms which absolute values of the jumps are between ϵ and 1. Two things can me said about this term; Firstly, It is not taken $\epsilon = 0$, rather than the limit, because υ can have a singularity. Secondly, the sum can have infinitely numbers, so to guarantee convergence it is necessary to center the distribution by subtracting its mean, $(\upsilon(dx))$, an use the first condition over the Lévy measure stated in the first point of the theorem.

Another form to uniquely define a Lévy process is by giving its characteristic function. The Lévy-Khinchin representation provides the expression for the characteristic function of a Lévy process, which is in terms of the associated characteristic triplet.

Theorem 2.7: ***Lévy-Khinchin representation [4]:*** *Let $(X_t)_{t\geq 0}$ a Lévy process on $\mathbb{R}^d$ with characteristic triplet (A, υ, γ). Then*

$$\mathbb{E}[e^{iz.X_t}] = e^{t\Psi(z)}, \qquad z \in \mathbb{R}^d \tag{2.2}$$

where

$$\Psi(z) = -\frac{1}{2}z.Az + i\gamma.z + \int_{\mathbb{R}^d}(e^{iz.x} - 1 - iz.x\mathbb{1}_{|x|\leq 1})\,\upsilon(dx). \tag{2.3}$$

2 Stable Distributions and Processes

While studying the returns or the volatility of a particular instrument, it is common to re-scale these measures to express them in years. For instance, if we have a sample with daily observations, the obtained volatility will be a *daily volatility*, and to annualize it we need to multiply it by $\sqrt{252}$. This is true because the returns are typically modeled with stable distributions. The normal distribution is an example of such distributions and it is probably the main reference while doing financial analysis; However, two of the main drawbacks of modeling using the normal distribution is its symmetry (skewness) and its absence of heavy tails (kurtosis).

To avoid these inconveniences it is possible to use other stable distributions, in this section it will be defined what is a stable distribution following [9] and later on it will be explained the link with Lévy processes, which is the main goal.

2.1 Stable Distributions

Definition 2.8: ***Stable Distribution [9]:*** *Let X a non-degenerate[5] random variable on $\mathbb{R}$. X is stable if and only if for all $n > 1$, there exist constants $c_n > 0$ and $d_n \in \mathbb{R}$ such that*

$$\sum_{i=1}^{n} X_n \overset{d}{=} c_n X + d_n, \tag{2.4}$$

where X_i with $i \in \{1, ...n, \}$ are independent, identical copies of X. X is strictly stable if and only if $d_n = 0$ for all n.

It can be proven that the only possible choice for the scaling constant is $c_n = n^{1/\alpha}$ for some $\alpha \in (0, 2]$. Nevertheless, since there are just few cases where an explicit formula of the density can be given for a stable distribution. It is necessary to give a definition where the characteristic function is stated. There are several parametrizations used in the literature. In this work, it will be stated the second parametrization given in [9], which is the same used in [4].

Definition 2.9: ***Stable Random Variable [9]:*** *Let X a non-degenerate random variable on $\mathbb{R}$ and $0 < \alpha \leq 2, -1 \leq \beta \leq 1, \gamma \neq 0, \delta \in \mathbb{R}$. X is stable if*

$$X \overset{d}{=} \begin{cases} \gamma Z + \delta & \alpha \neq 1 \\ \gamma Z + (\delta + \beta \frac{2}{\pi} \gamma log(\gamma)) & \alpha = 1, \end{cases} \tag{2.5}$$

where Z is a random variable with parameters (α, β). X has characteristic function

$$E(exp\{iuX\}) = \begin{cases} exp\{-\gamma^\alpha |u|^\alpha [1 - i\beta tan(\frac{\pi\alpha}{2}) sign(u)] + i\delta u\} & \alpha \neq 1 \\ exp\{-\gamma |u| [1 + i\beta \frac{2}{\pi} sign(u) log(|u|)] + i\delta u\} & \alpha = 1, \end{cases} \tag{2.6}$$

where $u \in \mathbb{R}$ and

$$sign(u) = \begin{cases} -1 & u < 0 \\ 0 & u = 0 \\ 1 & u > 0. \end{cases} \tag{2.7}$$

As we can see, there are four parameters that characterizes a distribution: an index of stability or characteristic exponent $\alpha \in (0, 2]$, a skewness parameter $\beta \in [-1, 1]$, a scale parameter $\gamma \geq 0$, and a location parameter $\delta \in \mathbb{R}$. α and β are considered the shape parameters because they determine the form of the distribution, and the distribution will be symmetric around zero when $\beta = 0$ and $\delta = 0$.

[5] X is a degenerate random variable if for some constant $a \in \mathbb{R}, \mathbb{P}(x = a) = 1$.

2.2 Stable Processes

Definition 2.8 is very similar to the selfsimilarity property for Lévy processes.

Proposition 2.10: ***Selfsimilarity of Lévy Processes [4]:*** *Let $(X_t)_{t\geq 0}$ a Lévy process on $\mathbb{R}^d$ with characteristic function $\Phi_{X_t}(z) = e^{-t\Psi(z)}$. X_t is called selfsimilar if*

$$\forall a > 0, \quad \exists b(a) > 0 : \quad \left(\frac{X_{at}}{b(a)}\right)_{t\geq 0} \stackrel{d}{=} (X_t)_{t\geq 0}. \tag{2.8}$$

or

$$\forall a > 0, \quad \exists b(a) > 0 : \quad \Phi_{X_t}(z)^a = \Phi_{X_t}(zb(a)) \quad \forall z. \tag{2.9}$$

It can be shown that the function $b(a) = a^{1/\alpha}$, where α is the stability index. If $a = n$, Equation (2.9) will be equal to c_n given in Equation (2.4), meaning that every selfsimilar Lévy process has a strictly stable distribution. When a Lévy process has stable distribution, we can observe a translation similar to the one in the Brownian motion.

$$\forall a > 0, \quad \exists c \in \mathbb{R}^d : \quad (X_{at})_{t\geq 0} \stackrel{d}{=} (a^{1/\alpha} X_t + ct)_{t\geq 0}. \tag{2.10}$$

This property justifies the "scaling" property described in the previous subsection for the Brownian motion. Another property of the Brownian motion that can be extended to Lévy processes is that the distribution associated with the process can be "split" infinitely, these type of distributions are called infinite divisible and they, for instance, give the possibility to simulate random paths to value path-dependent derivative instruments.

Definition 2.11: ***Infinite Divisible Distribution [4]:*** *A probability distribution F on $\mathbb{R}^d$ is said to be infinitely divisible if for any integer $n \geq 2$, there exists n i.i.d. random variables $Y_1, ...Y_n$ such that $Y_1 + ... + Y_n$ has distribution F.*

In fact, the following proposition states that given a Lévy process, it will always have an associated infinite divisible distribution and the opposite will also be true.

Proposition 2.12: ***Infinite divisibility and Lévy processes [4]:*** *Let $(X_t)_{t\geq 0}$ be a Lévy process. Then for every t, X_t has an infinitely divisible distribution. Conversely, if F is an infinitely divisible distribution then there exists a Lévy process (X_t) such that the distribution of X_1 is given by F.*

To finish this section, the next result gives the link between stable distributions and Lévy processes.

Proposition 2.13: ***Stable distribution and Lévy Processes [6]:*** *A distribution on $\mathbb{R}^d$ is α-stable with $0 < \alpha < 2$ if and only if it is infinitely divisible with characteristic triplet $(0, \upsilon, \gamma)$ and there exists a finite measure λ on S, a unit sphere of $\mathbb{R}^d$, such that*

$$\upsilon(B) = \int_S \lambda(d\xi) \int_0^\infty \mathbb{1}_B(r\xi) \frac{dr}{r^{1+\alpha}}. \tag{2.11}$$

3 Subordinated and Tempered Stable Processes

Merton's model described in [10], is one of the most known *jump-diffusion* models. The main property of these models is that only a finite number of jumps occurs in any bounded interval. It is possible to consider more general models with an infinite number of jumps in every interval and give a better, or at least more realistic, description of the price process, and even in some cases it is not necessary to introduce a Brownian component since the jumps are infinite in every interval. However, in this Section it will be mainly described two models that include this component via a technique called Brownian subordination.

Some advantages of the models with infinitely many jumps are given in [4], and are

- Do not necessarily contain a Brownian component.
- The process moves essentially by jumps.
- "Distribution of jump sizes" does not exist: jumps arrive infinitely often.
- Give a realistic description of the historical price process.
- Closed form densities available in some cases.
- In some cases can be represented via Brownian subordination, which gives additional tractability

Subordination is one of the three different ways to define a parametric Lévy process, the other two methods involve specifying the Lévy measure or the density of the increments. In this thesis it will be described the subordination technique, more details about the other two methods can be found in [4].

In simple terms, by subordination, a new Lévy process is obtained via a "composition" of two independent Lévy processes. That implies that one process (a subordinator) will randomly transform the time of another process giving as a result a new Lévy process which properties can be inferred from the properties of the subordinator.

Next subsection defines subordinators and then it will be explained the subordination of a Lévy Process.

3.1 Subordinators

A non-decreasing Lévy Processes is commonly referred as subordinators. Before specifying the requirements that a subordinator must meet, the following definitions are needed.

Proposition 2.14: ***Finite variation Lévy processes [4]:*** *A Lévy process is of finite variation* [6] *if and only if its characteristic triplet* (A, υ, γ) *satisfies:*

$$A = 0 \quad \text{and} \quad \int_{|x|\leq 1} |x|\, \upsilon(dx) < \infty. \tag{2.12}$$

This proposition provides the possibility to give particular expressions for the Lévy-Itô decomposition and the Lévy-Khinchin representation for Lévy processes with finite variation.

Proposition 2.15: ***Representation of finite variation Lévy processes [4]:*** *Let* $(X_t)_{t\geq 0}$ *a Lévy process of finite variation with Lévy triplet given by* $(\upsilon, 0, \gamma)$*. Then* X *can be expressed as the sum of jumps between* 0 *and* t *with a linear drift term:*

$$X_t = bt + \int_{[0,t]\times\mathbb{R}^d} x\, J_X(ds \times dx) = bt + \sum_{s\in[0,t]}^{\Delta X_s \neq 0} \Delta X_s, \tag{2.13}$$

[6] This means that for all the trajectories of the process, the total variation is finite with probability 1. Where the total variation of a function $f : [a, b] \to \mathbb{R}^d$ is defined by $TV(f) = sup \sum_{i=1}^{n} |f(t_i) - f(t_{i-1})|$, and the supremum is taken over all finite partitions in $[a, b]$

and its characteristic function can be expressed as:

$$\mathbb{E}[e^{iz.X_t}] = exp\left\{ t\left[ibz + \int_{\mathbb{R}^d} (e^{izx} - 1)\, \upsilon(dx) \right] \right\}, \tag{2.14}$$

where

$$b = \gamma - \int_{|x|\leq 1} x\, \upsilon(dx). \tag{2.15}$$

The previous representation will be very important for the next section. Now it is possible to introduce the conditions that characterize a subordinator.

Proposition 2.16: ***Increasing Lévy processes [4]:*** *Let $(X_t)_{t\geq 0}$ a Lévy process on $\mathbb{R}$. The following conditions are equivalent:*

- *$X_t \geq 0$ a.s. for some $t > 0$.*
- *$X_t \geq 0$ a.s. for every $t > 0$.*
- *Sample paths of (X_t) are almost surely non-decreasing: $t \geq s \Rightarrow X_t \geq X_s$ a.s.*
- *The characteristic triplet of (X_t) satisfies $A = 0, \upsilon((-\infty, 0]) = 0, \int_0^\infty (x \wedge 1)\, \upsilon(dx) < \infty$ and $b \geq 0$, that is, (X_t) has no diffusion component, only positive jumps of finite variation and positive drift.*

3.2 Subordination

For this technique, it is necessary to start with a subordinator, i.e. an increasing Lévy process $(S_t)_{t\geq 0}$. Since S_t is a positive random variable for all t, it is possible to describe it using the Laplace transform.

The Laplace transform[7] of a random variable S is defined as

$$\mathscr{L}\{u\} = \mathbb{E}[e^{-uS_t}]. \tag{2.16}$$

According to the last point in Definition 2.16, lets assume that S_t has the characteristic triplet $(0, \rho, b)$. Then the Laplace transform is given by

$$\mathbb{E}[e^{-uS_t}] = exp\left\{ t\left[\int_0^\infty (e^{-ux} - 1)\, \rho(dx) - bu \right] \right\}, \qquad \forall u \geq 0. \tag{2.17}$$

Note that it is a particular case of Equation (2.14). Therefore, the moment generating function of S_t can be expressed as

$$\mathbb{E}[e^{-uS_t}] = e^{l(u)} \qquad \forall u \geq 0, \qquad \text{where} \qquad l(u) = bu + \int_0^\infty (e^{ux} - 1)\, \rho(dx). \tag{2.18}$$

$l(u)$ is called the Laplace exponent of S_t. With this representation and having in mind the characteristic function of a Lévy procees, it is possible to give the next result.

Theorem 2.17: ***Subordination of a Lévy process [4]:*** *Fix a probability space $(\Omega, \mathcal{F}, \mathbb{P})$. Let $(X_t)_{t\geq 0}$ a Lévy process on $\mathbb{R}^d$ with characteristic exponent $\Psi(u)$ and triplet (A, υ, γ) and let $(S_t)_{t\geq 0}$ be a subordinator with Laplace exponent $l(u)$ and triplet $(0, \rho, b)$. Then the process $(Y_t)_{t\geq 0}$ defined for each $\omega \in \Omega$ by $Y(t, \omega) = X(S(t, \omega), \omega)$ is a Lévy process. Its characteristic function is*

$$\mathbb{E}[e^{iuY_t}] = e^{tl(\Psi(u))},$$

[7] The Laplace transform uniquely determine the distribution of a random variable but it does not always exist. It exist for positive random variables that does not have heavy tails.

i.e., the characteristic exponent of Y is obtained by composition of the Laplace exponent of S with the characteristic exponent of X. The triplet $(A^Y, \upsilon^Y, \gamma^Y)$ of Y is given by

$$\begin{aligned} A^Y &= bA, \\ \upsilon^Y(B) &= b\upsilon(B) + \int_0^\infty p_s^X(B)\,\rho(ds) \quad \forall B \in \mathcal{B}(\mathbb{R}^d), \\ \gamma^Y &= b\gamma + \int_0^\infty \rho(ds) \int_{|x|\leq 1} x p_s^X(B)\,(dx), \end{aligned} \tag{2.19}$$

where $p_s^X(B)$ is the probability distribution of X_t.

The transformation of the process $(X_t)_{t\geq 0}$ to $(Y_t)_{t\geq 0}$ is called subordination by the process $(S_t)_{t\geq 0}$ and $(Y_t)_{t\geq 0}$ is said to be subordinate to the process $(X_t)_{t\geq 0}$.

When the process $(X_t)_{t\geq 0}$ is a stable process, it produces a particular class of subordinators.

Proposition 2.18: ***Stable processes and subordinators [4]:*** *Let $(S_t)_{t>0}$ a stable process on $\mathbb{R}$ with parameters $(\alpha, \gamma, \beta, \delta)$. S_t is a subordinator if and only if $0 < \alpha < 1, \beta = 1$ and $\delta \geq 0$. The process S_t is called a stable subordinator.*

3.3 Brownian Subordination

As the name says, Brownian subordination will have two associated elements: a Brownian motion with drift μ, that is $(B_t)_{t\geq 0} = (\mu t + W_t)_{t\geq 0}$, and a subordinator, $(S_t)_{t\geq 0}$, with Laplace exponent $l(u)$. Following the notation in Theorem 2.17, $(B_t)_{t\geq 0}$ would be $(X_t)_{t\geq 0}$, and the new process $(Y_t)_{t\geq 0}$ will take the form

$$Y_t = B_{S_t} = \mu S_t + W_{S_t}. \tag{2.20}$$

This sort of composition substitutes from the Brownian motion the deterministic time t with a random variable S_t. Therefore, the Brownian motion will have a new (stochastic) time scale given by S_t.

Next theorem will give some conditions that the Lévy measure needs to fulfill for the new process obtained by Brownian subordination.

Theorem 2.19: ***Lévy measure and Brownian subordination [4]:*** *Let υ be a Lévy measure on $\mathbb{R}$ and $\mu \in \mathbb{R}$. There exists a process $(Y_t)_{t\geq 0}$ with Lévy measure υ such that $Y_t = \mu S_t + W_{S_t}$ for some subordinator $(S_t)_{t\geq 0}$ and some Winner process $(W_t)_{t\geq 0}$ independent from S_t if and only if the following conditions are satisfied:*

1. *υ is absolutely continuous[8] with density $v(x)$.*
2. *$v(x)e^{-\mu x} = v(-x)e^{\mu x}$.*
3. *$v(\sqrt{u})e^{-\mu\sqrt{u}}$ is a completely monotonic function[9] on $(0, \infty)$.*

The first thing that can be observed is that the Lévy measure is multiplied by an exponential function and it satisfies some properties. The multiplication of a Lévy measure by an exponential function has a particular name given as follows

Proposition 2.20: ***Exponential titling of Lévy measures [4]:*** *Let υ be a Lévy measure on $\mathbb{R}^d$. If there exist $\mu \in \mathbb{R}^d$ such that $\int_{|x|\geq 1} e^{\mu x}\upsilon(dx) < \infty$ then the measure $\tilde{\upsilon}$ defined by*

$$\tilde{\upsilon}(dx) := e^{\mu x}\upsilon(dx), \tag{2.21}$$

is a Lévy measure.

[8] A function $f : [a, b] \to \mathbb{R}$ is called absolutely continuous if for every $\epsilon > 0$, there exist a $\delta > 0$ so that if any finite set of disjoint intervals $\{(a_i, b_i)\}_{i=1,\ldots n.}$ of $[a, b]$ satisfies $\sum_{i=1}^n (a_i - b_i) < \delta$, then $\sum_{i=1}^n |f(a_i) - f(b_i)| < \epsilon$.

[9] A function $f : [a, b] \to \mathbb{R}$ is called completely monotonic if all its derivatives exist and $(-1)^k \frac{\partial^k f(u)}{\partial u^k > 0}$ for all $k \geq 1$.

Transforming the Lévy measure of any process, lets say $(X_t)_{t\geq 0}$, with an exponential will not affect the other two elements of its characteristic triplet, and the new Lévy process is called the Esscher transform of X. By setting a Lévy measure, the jump structure of a process is being described. Theorem 2.19 says that if the Lévy measure fulfill the three stated conditions, the process can be represented as a Brownian motion with a stochastic time scale.

3.4 Tempered Stable Processes

A tempered stable process is created by taking a stable process on $\mathbb{R}$ and multiplying its Lévy measure with a decreasing exponential function on each half of the real axis. With this transformation, each tail will experiment an exponential softening given particular parameters. According to Proposition 2.13, a tempered stable process is a Lévy process on $\mathbb{R}$ with no Gaussian component and Lévy measure

$$\upsilon(x) = \frac{c_-}{|x|^{1+\alpha}} e^{-\lambda_- |x|} \mathbb{1}_{x<0} + \frac{c_+}{x^{1+\alpha}} e^{-\lambda_+ x} \mathbb{1}_{x>0}, \tag{2.22}$$

where the parameters satisfy $c_- > 0, c_+ > 0, \lambda_- > 0, \lambda_+ > 0$ and $\alpha < 2$. c_- and c_+ are constants that alters the intensity of all jumps, so they change the time scale of the process, λ_- and λ_+ will set the decay rate of (mainly) big jumps, and α will determine the relative importance of small jumps in the path of the process. It is possible to define tempered stable processes for $\alpha < 0$, more details and properties of these processes can be found in [9].

As a special case, a tampered stable subordinator will only consider the positive tail, so they will have two parameters c, λ. These processes have also a scaling property which is stated in the next proposition.

Proposition 2.21: ***Scaling property of tempered stable subordinators [4]:*** *Let $(S_t(\alpha, \lambda, c))_{t\geq 0}$ be a tempered stable subordiator with parameters α, λ and c. Then for every $r > 0$, $rS_t(\alpha, \lambda, c)$ has the same law as $S_{r^\alpha t}(\alpha, \lambda/r, c)$.*

This property, in combination with the selfsimilarity of the Brownian motion, implies that for subordinated models, it is sufficient to consider only tempered stable subordinators with $\mathbb{E}[S_t] = t$, which form a two-parameter family. Following the parametrization in [4], it is possible to define tempered stable subordinators.

Proposition 2.22: ***Tampered stable subordinators [4]:*** *Let $(S_t)_{t\geq 0}$ a tempered stable subordinator on $\mathbb{R}$ with parameters (α, κ) and characteristic triplet $(0, \rho, b)$. The Lévy measure of S is given by*

$$\rho(x) = \frac{1}{\Gamma(1-\alpha)} \left(\frac{1-\alpha}{\kappa}\right)^{1-\alpha} \frac{e^{-(1-\alpha)x/\kappa}}{x^{1+\alpha}}, \tag{2.23}$$

where α is the index of stability, $\alpha \in [0, 1)$ and κ is the variance of the subordinator at time 1. And the Laplace transform of $(S_t)_{t\geq 0}$ is

$$l(u) = \begin{cases} \frac{t}{\kappa}\frac{1-\alpha}{\alpha}\left\{1 - \left(1 + \frac{u\kappa}{1-\alpha}\right)^{\alpha}\right\} & 0 < \alpha < 1 \\ -\frac{t}{\kappa} log(1 + u\kappa) & \alpha = 0. \end{cases} \tag{2.24}$$

In this case, κ will determine how random the time change will be, and when $\kappa = 0$, it corresponds to a deterministic function.

The difficulty with stable processes is that the density does not always exist. In fact, it only exists when $\alpha = 0$ or $\alpha = 1/2$, defining the Gamma and the Inverse Gaussian subordinators, respectively.

4 Normal Tempered Stable Processes

A LTS process is obtained when the Brownian subordination is performed using a tempered stable subordinator[10]. In this section, it will be discussed some general properties of LTS processes and the two main examples of such processes, the Variance Gamma (VG) process and the Normal Inverse Gaussian (NIG) process.

LTS processes are subject to four parameters:

- α: index of stability.
- μ: drift of the Brownian motion.
- σ: volatility of the Brownian motion.
- κ: variance of the subordinator.

The characteristic function is obtained by applying Theorem 2.17, where the characteristic exponent of the Brownian process, which is $i\mu - \sigma^2/2$, is evaluated in the Laplace exponent of S_t given in Equation (2.24). This give us the expression

$$\mathbb{E}[e^{iuX_t}] = \mathscr{L}_t\left(iu\mu - \frac{u^2\sigma^2}{2}; \kappa; \alpha\right), \tag{2.25}$$

where $\log(\mathscr{L}_t(u;\kappa;\alpha)) := l(u)$ and the conditions in Proposition 2.22 are fulfilled.

The Lévy measure of these processes will have the general form

$$\upsilon(x) = \frac{C(\alpha,\kappa,\sigma,\mu)}{|x|^{\alpha+1/2}} e^{\mu x/\sigma^2} K_{\alpha+1/2}\left(\frac{|x|\sqrt{\mu^2 + \frac{2}{\kappa}\sigma^2(1-\alpha)}}{\sigma^2}\right), \tag{2.26}$$

where

$$C(\alpha,\kappa,\sigma,\mu) = \frac{2}{\Gamma(1-\alpha)\sigma\sqrt{2\pi}}\left(\frac{1-\alpha}{\kappa}\right)^{1-\alpha}\left(\mu^2 + \frac{2}{\kappa}\sigma^2(1-\alpha)\right)^{\frac{\alpha}{2}+\frac{1}{4}} \tag{2.27}$$

and K is the the modified Bassel function of the second kind[11].

The behavior of the Lévy measure in the tails and in the center of the distribution can be deduced by using the asymptotic behavior of K

$$\begin{aligned} \upsilon(x) &\sim \frac{1}{|x|^{2\alpha+1}}, \quad \text{when} \quad x \to 0, \\ \upsilon(x) &\sim \frac{1}{|x|^{\alpha+1}} e^{-\lambda_+ x}, \quad \text{when} \quad x \to \infty, \\ \upsilon(x) &\sim \frac{1}{|x|^{\alpha+1}} e^{-\lambda_- |x|}, \quad \text{when} \quad x \to -\infty. \end{aligned} \tag{2.28}$$

The previous implies that the Lévy measure has stable-like behavior near zero and exponential decay with decay rates λ_+ and λ_- at the tails.

[10] In general, when a process is obtained via Brownian subordination, it is common to write the word "normal" before the properties of the subordinator.

[11] This function is defined as the solution that is bounded when $z \to \infty$ of the differential equation $z^2\frac{\partial^2 w}{\partial z^2} + z\frac{\partial w}{\partial z} - (z^2 + v^2)w = 0$ where $z \geq 0$ and $v \geq 0$.

4.1 The Variance Gamma Process

The VG process is obtained via Brownian subordination where the subordinator is a Gamma process. That means that the time of the Brownian motion will be given by a Gamma process. The VG process was studied in [2] as a generalization of the symmetric VG process studied by the same authors years earlier. To understand this process, first will be defined the Gamma process.

Definition 2.23: ***Gamma Process [2]:*** *Let $(S_t)_{t\geq 0}$ a process on $\mathbb{R}^+$. S_t is a Gamma process with parameters $a > 0$ and $b > 0$, when the density function at time t is given by*

$$f_{S_t}(x) = \frac{b^{at}}{\Gamma(at)} x^{at-1} e^{-bx}. \tag{2.29}$$

With this parametrization, a is considered the shape parameter and b the rate parameter. To avoid confusion, it would be helpful to use the same notation for the parameters as in the previous subsection; However, Definition 2.23 contemplates two parameters while the only parameter considered for the subordinator was κ. That is because it can be assumed that the parameters take the form: $a = 1/\kappa$ and $b = 1/\kappa$. By defining the parameters in this way, it can be verified that the mean of the subordinator is $a/b = 1$ and the variance is $a/b^2 = \kappa$.

By changing the parameters in Equation (2.29) for the ones proposed above, the density function of the Gamma process is now given by

$$f_{S_t}(x) = \frac{\kappa^{-\frac{t}{\kappa}}}{\Gamma(\frac{t}{\kappa})} x^{\frac{t}{\kappa}-1} e^{-\frac{x}{\kappa}}. \tag{2.30}$$

Using Equation (2.23), and by knowing that for the Gamma process, $\alpha = 0$, the Lévy measure of this process is

$$\rho(x) = \frac{1}{\kappa} \frac{e^{-x/\kappa}}{x}. \tag{2.31}$$

Coming back to the VG process, its Lévy measure can give an idea of how the skewness and kurtosis of the distribution is controlled by the parameters μ and κ, respectively. The Lévy measure of the VG process is

$$\upsilon(x) = \frac{e^{\frac{\mu x}{\sigma^2}}}{\kappa|x|} \exp\left(-\frac{\sqrt{\frac{2}{\kappa} + \frac{\mu^2}{\sigma^2}}}{\sigma} |x| \right). \tag{2.32}$$

If $\mu = 0$, the Lévy measure is symmetric around zero, so positive and negative values will appear in the same proportion. If $\mu < 0$, negative values of the process will appear with a higher probability and the distribution will present negative skewness and the opposite will happen if $\mu > 0$. On the other hand, large values of κ will make that the exponential decay rate (right exponential) will be less violent over the tails, so large jumps will occur with higher probability and hence the kurtosis will increase.

In [4] it is possible to find the density function of the VG process expressed in terms of the modified Bassel function of the second kind, that is

$$f_{X_t}(x) = C|x|^{\frac{t}{k}-\frac{1}{2}} e^{Ax} K_{\frac{t}{k}-\frac{1}{2}}(B|x|), \tag{2.33}$$

where

$$A = \frac{\mu}{\sigma^2}, \qquad B = \frac{\sqrt{\mu^2 + 2\sigma^2/\kappa}}{\sigma^2}, \qquad C = \sqrt{\frac{\sigma^2\kappa}{2\pi}} \frac{(\mu^2\kappa + 2\sigma^2)^{\frac{1}{4}-\frac{\mu}{2\kappa}}}{\Gamma(t/\kappa)}.$$

Finally, the characteristic function and the first four central moments of the VG process at time t are given by

$$\Phi_{X_t}(u) = \left(\frac{1}{1 - i\mu\kappa u + (\sigma^2\kappa/2)u^2)} \right)^{\frac{t}{\kappa}}, \tag{2.34}$$

$$\begin{aligned}\mathbb{E}[X_t] &= \mu t,\\ \mathbb{E}[(X_t-\mathbb{E}[X_t])^2] &= (\mu^2\kappa+\sigma^2)t,\\ \mathbb{E}[(X_t-\mathbb{E}[X_t])^3] &= (2\mu^3\kappa^2+3\sigma^2\mu\kappa)t,\\ \mathbb{E}[(X_t-\mathbb{E}[X_t])^4] &= (3\sigma^4\kappa+6\mu^4\kappa^3+12\sigma^2\mu^2\kappa^2)t.\end{aligned}$$

The VG process has paths of finite variation and it is possible to obtain this process by a difference of two independent Gamma processes. In [2] it is described how to price plain vanilla instruments by following a probabilistic approach; However, a different technique will be used to price derivatives under this model.

4.2 The Normal Inverse Gaussian Process

The NIG process is obtained via Brownian subordination where the subordinator is an Inverse Gaussian (IG) process. This process and its applications in finance were studied in [3] and [11], and it was shown that it captures realistic features that are observed in the market; For instance, some of the properties of this process are: it can be asymmetric, it captures conditional heteroscedasticity, the normal density is obtained as a limit case and it has the scaling property that was discussed in Proposition 2.21.

In general, Brownian subordination is not the only method[12] to obtain the NIG process, and depending on the approach that is used, it is common to have different parametrizations for the IG process and the NIG process. In this thesis, [11] will be followed to define the IG process.

Definition 2.24: ***Inverse Gaussian Process [11]:*** *Let $(S_t)_{t\geq 0}$ a process on $\mathbb{R}^+$. S_t is an IG process with parameters $\delta>0$ and $\gamma>0$) when the density function at time t is given by*

$$f_{S_t}(x)=\frac{\delta t e^{t\delta\gamma}}{\sqrt{2\pi x^3}}e^{-\frac{1}{2}\left(\frac{t^2\delta^2}{x}+\gamma^2 x\right)}. \tag{2.35}$$

The two parameters δ,γ controls the shape and scale of the distribution, respectively. The IG process can also be interpreted as the first passage time of a Brownian motion with drift $\gamma>0$ and diffusion 1 for a fixed level $\delta t>0$. The previous can be written as $S_t=inf\{s>0|B_s=\delta t\}$.

If we consider a Brownian motion that starts at ξ, with drift β, independent from S_t, and if we set $\alpha=\sqrt{\beta^2+\gamma^2}$, a new process Y_t defined as

$$Y_t=\beta S_t+W_{S_t}+\xi t \tag{2.36}$$

will be distributed as the NIG process with parameters $(\alpha,\beta,\xi,\delta)$ for $t=1$, where the conditions of the parameters are $0<|\beta|\leq\alpha,\xi\in\mathbb{R}$ and $0<\delta$. To interpret the parameters, they can be divided in two groups, the first corresponds to α and β and it controls the shape, while the second group corresponds to ξ and δ and it controls the location and scale of the distribution. In this sense, α refers to the flatness of the distribution that will be located around ξ, β will control the skewness and δ will control how narrow or wider the distribution will be.

Until now, the NIG process has been represented with four parameters; However, in the following it will be assumed that $\xi=0$, so the NIG process will always be centered at 0.

To express the density in Equation (2.35) in terms of the the parameter κ, it is possible to set $\delta=1/\sqrt{\kappa}$ and $\gamma=1/\sqrt{\kappa}$, this parametrization is the same given in [4] and has the next form

$$f_{S_t}(x)=\frac{te^{\frac{t}{\kappa}}}{\sqrt{2\pi\kappa x^3}}e^{-\frac{1}{2\kappa}\left(\frac{t^2}{x}+x\right)}. \tag{2.37}$$

[12]The NIG process can also be obtained with a normal variance-mean mixture distribution, where the NIG at $t=1$ corresponds to the conditional distribution $X|Z$, which is distributed $N(\mu+\beta z,z)$ where Z follows a $IG(\delta,\sqrt{\alpha^2+\beta^2})$ for $|\beta|\leq\alpha$.

Having the density with this representation, it can be shown that the expectation of the subordinator is 1, because $\mathbb{E}[S_t] = \delta/\gamma = (1/\sqrt{\kappa})/(1/\sqrt{\kappa}) = 1$ and the variance is $Var(S_t]) = \delta/\gamma^3 = \kappa^{-\frac{1}{2}}/\kappa^{-\frac{3}{2}} = \kappa$. Furthermore, the Lévy density for the IG is a particular case of Equation (2.23), when $\alpha = 1$, and it is given by

$$\rho(x) = \frac{1}{\sqrt{2\pi\kappa}} - \frac{e^{\frac{x}{2\kappa}}}{x^{3/2}}. \tag{2.38}$$

On the other hand, the probability density and the Lévy measure of the NIG process are given by

$$f_{X_t}(x) = Ce^{Ax}\frac{K_1(B\sqrt{x^2 + t^2\sigma^2/\kappa})}{\sqrt{x^2 + t^2\sigma^2/\kappa}}, \tag{2.39}$$

$$\upsilon(x) = \frac{\sqrt{\mu^2 + \sigma^2/\kappa}}{2|x|\pi\sigma\sqrt{\kappa}}e^{Ax}K_1(B|x|), \tag{2.40}$$

where

$$A = \frac{\mu}{\sigma^2}, \qquad B = \frac{\sqrt{\mu^2 + \sigma^2/\kappa}}{\sigma^2}, \qquad C = \frac{t}{\pi}e^{\frac{t}{k}}\sqrt{\frac{\mu^2}{\kappa\sigma^2} + \frac{1}{\kappa^2}}.$$

Finally, the first four central moments at time t are expressed as follows

$$\begin{aligned}
\mathbb{E}[X_t] = &\quad \mu t,\\
\mathbb{E}[(X_t - \mathbb{E}[X_t])^2] = &\quad (\mu^2\kappa + \sigma^2)t,\\
\mathbb{E}[(X_t - \mathbb{E}[X_t])^3] = &\quad (2\mu^3\kappa^2 + 3\sigma^2\mu\kappa)t,\\
\mathbb{E}[(X_t - \mathbb{E}[X_t])^4] = &\quad (3\sigma^4\kappa + 15\mu^4\kappa^3 + 18\sigma^2\mu^2\kappa^2).
\end{aligned}$$

The VG process and the NIG process are pure jumpe processes, i.e., in their characteristics triplets, $A = 0$; However, their nature of jumps are different because the VG process has finite variation, while the NIG process has infinite variation as the Brownian motion. Another similarity between both processes is that when the variance of the time change tends to zero, both processes approximate the Brownian motion process. Finally, both processes has the so called semi-heavy tails, this means that the Lévy measure and the probability density have exponential tails with decay rates $\lambda_+ = B - A$ and $\lambda_- = B + A$, where B, A are defined in its corresponding subsection.

5 Additive Normal Tempered Stable Processes

Time inhomogeneous jump processes are defined in a similar way as Lévy processes with the difference that their increments do not need to be stationary. This helps to model some properties that are observed in the market and that were mentioned in the introduction; However, these type of processes are rather general and have been studied for particular applications. This thesis will focus in the subclass of time inhomogeneous processes that were studied in [5], and that the authors called ATS processes.

The main property of ATS processes is that they will have deterministic and time-dependent parameters, and given a fixed time t, a Lévy process can be associated, allowing to preserve all the properties that have been studied in previous sections.

The aim of this section is to define additive processes following [4], and establish the relationship between ATS and LTS processes that was proven in [5].

5.1 Additive Processes

Definition 2.25: ***Additive Process [4]:*** *A stochastic process $(X_t)_{t\geq 0}$ on $\mathbb{R}^d$ is called an additive process if it is cadlag, satisfies $X_0 = 0$ and possesses the following properties:*

1. *Independent increments: for every increasing sequence of times $t_0, ..., t_n$, the random variables $X_{t_0}, X_{t_1} - X_{t_0}, ..., X_{t_n} - X_{t_{n-1}}$ are independent.*
2. *Stochastic continuity: $\forall \epsilon > 0$, $\lim_{h\to 0} P(|X_{t+h} - X_t| \geq \epsilon) = 0$.*

One important property of these processes is that for each t, every additive process, X_t, has associated an infinitely divisible distribution. In Section 1, it was explained that every Lévy process can be fully represented with a characteristic triplet. In the case of additive processes, something similar happens, every additive process has an associated characteristic triplet with the particularity that the elements in the triplet are time-dependent.

Following the notation in [4], the triplet of an additive process X_t is given by $(A_t, \upsilon_t, \gamma_t)$, where A_t is the covariance matrix of a Brownian motion at time t, υ_t is the Lévy measure at time t and γ_t is the drift at time t. In this case $(A_t, \upsilon_t, \gamma_t)$ is called the characteristic triplet of X.

5.2 ATS Processes

In Section 4, it was mentioned that LTS are subject to four parameters, α, μ, σ and, κ. The authors in [5] proposed a model with a particular expression for μ that allows to control the skew of the volatility smile of a given maturity. The proposed model is

$$f_t = -\left(\frac{1}{2} + \eta\right)\sigma^2 S_t + \sigma W_{S_t} + \rho t, \qquad \forall t \in [0, T]. \tag{2.41}$$

In this case, X_t is now called f_t and $\mu = (\frac{1}{2} + \eta)\sigma^2$. It is also included another parameter, ρ, but in the next chapter it will be explained its financial interpretation and for now the value of this parameter will be assumed fixed.

Using Equation (2.25), the characteristic function of the process f_t will have the form

$$\mathbb{E}[e^{iuf_t}] = \mathscr{L}_t\left(iu\left(\frac{1}{2} + \eta\right)\sigma^2 + \frac{u^2\sigma^2}{2}; \kappa; \alpha\right) e^{iu\rho t}, \tag{2.42}$$

where $\alpha \in [0, 1)$ and

$$\log(\mathscr{L}_t(u; \kappa; \alpha)) = \begin{cases} \frac{t}{\kappa}\frac{1-\alpha}{\alpha}\left\{1 - \left(1 + \frac{u\kappa}{1-\alpha}\right)^{\alpha}\right\} & 0 < \alpha < 1 \\ -\frac{t}{\kappa}\log(1 + u\kappa) & \alpha = 0. \end{cases} \tag{2.43}$$

Once this LTS is fully described, it was proved that there is associated an additive process with the same characteristic function but with time-dependent parameters if some conditions are fulfilled. The characteristic function will take the form

$$\mathbb{E}[e^{iuf_t}] = \mathscr{L}_t\left(iu\left(\frac{1}{2}+\eta_t\right)\sigma_t^2 + \frac{u^2\sigma_t^2}{2}; \kappa_t; \alpha\right)e^{iu\rho_t t}, \tag{2.44}$$

where $\alpha \in [0,1)$, σ_t, κ_t are continuous on $[0,\infty)$ and η_t, ρ_t are continuous on $[0,\infty)$ with $\sigma_t > 0, \kappa \geq 0$ and $\rho_t t$ goes to zero as t goes to zero.

The conditions for existence of the associated additive process with characteristic function given in Equation (2.44) are stated in Theorem 2.1 in [5], these conditions are

1. $g_1(t), g_2(t)$ and $g_3(t)$ are non decreasing, where

$$\begin{aligned} g_1(t) &:= \left(\frac{1}{2}+\eta_t\right) - \sqrt{\left(\frac{1}{2}+\eta_t\right)^2 + \frac{2(1-\alpha)}{\sigma_t^2\kappa_t}}, \\ g_2(t) &:= -\left(\frac{1}{2}+\eta_t\right) - \sqrt{\left(\frac{1}{2}+\eta_t\right)^2 + \frac{2(1-\alpha)}{\sigma_t^2\kappa_t}}, \\ g_3(t) &:= \frac{t^{1/\alpha}\sigma_t^2}{\kappa_t^{(1-\alpha)/\alpha}}\sqrt{\left(\frac{1}{2}+\eta_t\right)^2 + \frac{2(1-\alpha)}{\sigma_t^2\kappa_t}}. \end{aligned}$$

2. Both $t\sigma_t^2\eta_t$ and $\frac{t\sigma_t^{2\alpha}\eta_t^\alpha}{\kappa_t^{1-\alpha}}$ go to zero as t goes to zero.

Since the conditions are too general, these processes were studied for a particularly sub-case where the parameters η_t and κ_t follows a power-law scalling property and σ is constant. The proof of this result is given in Theorem 2.3 in [5] and it states that there exist as ATS with parameters

$$\kappa_t = \bar{\kappa}t^\beta, \qquad \eta_t = \bar{\eta}t^\delta, \qquad \sigma_t = \bar{\sigma},$$

where $\alpha \in [0,1)$, $\bar{\sigma}, \bar{\eta}, \bar{\kappa} \in \mathbb{R}^+$ and $\beta, \delta \in \mathbb{R}$ satisfy the following conditions

1. $0 \leq \beta \leq \frac{1}{1-\alpha/2}$,
2. -min$\left(\beta, \frac{1-\beta(1-\alpha}{\alpha}\right) \leq \delta \leq 0$,
   where this condition reduces to $-\beta < \delta \leq 0$ for $\alpha = 0$.

Considering the parameters in this way, and if $\beta = 0$ and $\alpha = 0$, a LTS process is recovered loosing the additive property.

Now that the ATS processes have been defined and the relationship with the LTS processes has been stated, in the next chapter the model that will be used to price derivative instruments will be described in detail.

Chapter 3

Model Implementation

1 Model Description

To describe the evolution of an asset price in the Black-Scholes model, two things are needed: the asset price at time $t = 0$ and a geometric Brownian motion. In ATS processes, a similar idea is followed with the difference that the underlying asset will be the corresponding forward price with maturity at time T, expressed as $F_t(T)$, and instead of the geometric Brownian motion, it will be taken the exponential of the ATS process expressed by f_t given in Equation 2.41. Therefore, the model is given by

$$F_t(T) := F_0(T)\exp(f_t), \tag{3.1}$$

where

$$f_t = -\left(\frac{1}{2} + \eta_t\right)\sigma_t^2 S_t + \sigma_t W_{S_t} + \rho_t t, \qquad \forall t \in [0, T]$$

and $\kappa_t, \eta_t, \sigma_t$ follow the power-law scaling of ATS, that is, $\kappa_t = \bar{\kappa}t^{\beta}, \eta_t = \bar{\eta}t^{\delta}$, and $\sigma_t = \bar{\sigma}$.

The domain and a short description of each parameter is given as follows

- $\bar{\eta} \in \mathbb{R}^+$, controls the skew of the smile.
- $\bar{\kappa} \in \mathbb{R}^+$, volatility of the subordinator (volatility of the volatility).
- $\bar{\sigma} \in \mathbb{R}^+$, average volatility.
- $\alpha \in [0, 1)$, index of stability.
- $\beta \in \left[0, \frac{1}{1-\alpha/2}\right]$ power-law scaling parameter of κ (affects the variance of jumps).
- $\delta \in \left[-\min\left(\beta, \frac{1-\beta(1-\alpha}{\alpha}\right), 0\right]$ power-law scaling parameter of η (affects the smile asymmetry).
- $\rho_t \in \mathbb{R}$ parameter that will make the model martingale.

Even though there are seven parameters that describe the model, during the calibration process that will be explained in further sections, only the parameters $\bar{\eta}, \bar{\kappa}$ and $\bar{\sigma}$ will be found. The index of stability, α, will be fix and it will be considered the cases where $\alpha = 0$ and $\alpha = 1/2$, to analyze the VG and NIG processes, respectively.

For the parameters β and δ, it will be assumed that $\beta = 1$ and $\delta = -0.5$. The previous values are justified by Theorem 5.1 in [12], which states that the implied volatility of ATS processes is consistent in the short time with the equity market empirical characteristics if and only if $\beta = 1$ and $\delta = -0.5$. Such empirical characteristics refers to the empirical studies that have shown that the equity implied volatility has a negative skew which is proportional to the inverse of the square root of the time-to-maturity.

Finally, ρ_t, and in particular the product $\rho_t t$, will be chosen in a way that, for any time t, the process $F_t(T)$ satisfies the martingale property, which means that $\mathbb{E}[F_t(T)|\mathcal{F}_0] = F_0(T)$. Proposition 2.2 in [5] states that the martingale property is fulfilled if and only if

$$\rho_t t = -\log(\mathscr{L}_t(\sigma_t^2 \eta_t; \kappa_t; \alpha)), \tag{3.2}$$

where $\log(\mathscr{L}_t(.))$ is given in Equation (2.43).

Since the "fixed" values of the model's parameters has been explained, it is possible to describe how the other three parameters, $\bar{\eta}, \bar{\kappa}$ and $\bar{\sigma}$, will affect the shape of the volatility smile for a given maturity.

For the parameter $\bar{\eta}$, Figure 3.1 shows how it controls the skew of the volatility smile, the bigger the parameter $\bar{\eta}$, the bigger the volatility skew. Additionally, it can be proved that when $\bar{\eta} = 0$, the smile is symmetric [13].

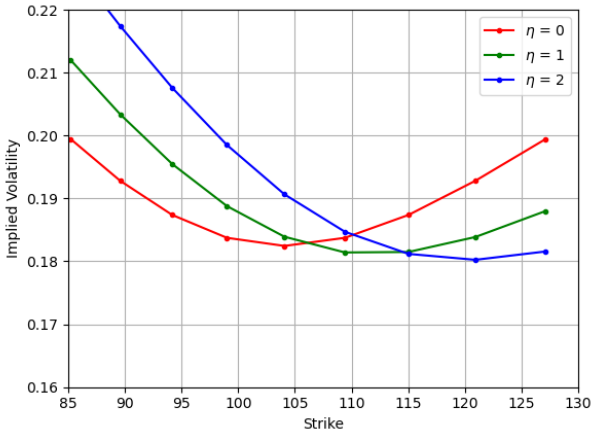

Figure 3.1: Implied volatility of a call option for different values of $\bar{\eta}$. The rest of the parameters remains constant with values: $\bar{\kappa} = 1, \bar{\sigma} = .2, \alpha = 1/2, \beta = 1, \delta = -0.5, S_0 = 100, r = .04, T = 1$.

In Figure 3.2, the parameter $\bar{\kappa}$ shows how the volatility of the subordinator affects the volatility smile. This parameter is considered as the volatility of the volatility.

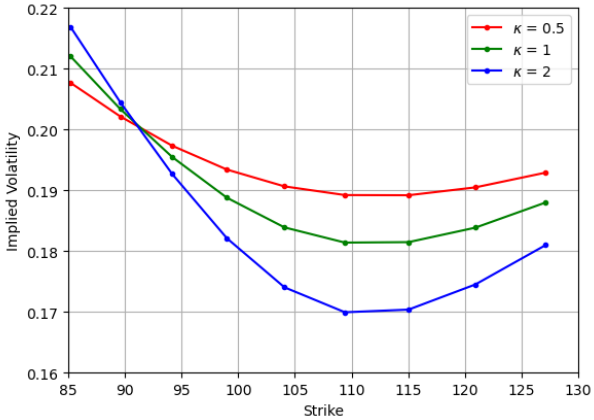

Figure 3.2: Implied volatility of a call option for different values of $\bar{\kappa}$. The rest of the parameters remains constant with values: $\bar{\eta} = 1, \bar{\sigma} = .2, \alpha = 1/2, \beta = 1, \delta = -0.5, S_0 = 100, r = .04, T = 1$.

Finally, in Figure 3.3 it is possible to observe how the parameter $\bar{\sigma}$ affects the average level of the volatility smile.

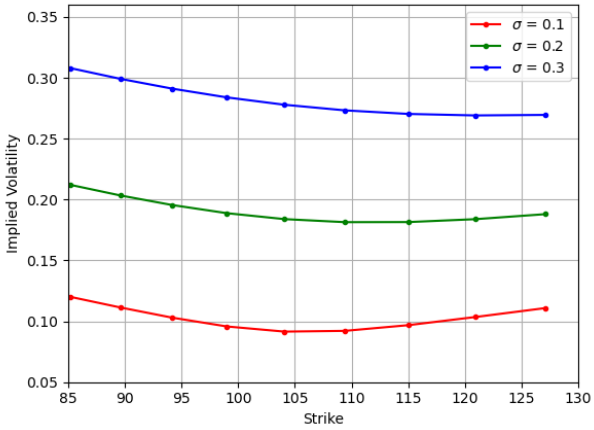

Figure 3.3: Implied volatility of a call option for different values of $\bar{\sigma}$. The rest of the parameters remains constant with values: $\bar{\eta} = 1, \bar{\kappa} = 1, \alpha = 1/2, \beta = 1, \delta = -0.5, S_0 = 100, r = .04, T = 1$.

2 Option Valuation using the Fast Fourier Transform

To price European options considering ATS processes, the Fourier based approach is an excellent alternative since the main requirement to use this method is the characteristic function of the model, which was presented in Equation 2.42. In particular, the Lewis formula studied in [14] will be used to price European call options since the analysis of the thesis will be carried out on this type of options.

2.1 Fourier Transform

Before stating the Lewis formula, it is necessary to define the Fourier Transform (FT).

Definition 3.1: ***Fourier Transform [15]:*** *The FT of $f(x)$ is defined as*

$$\mathcal{F}[f](x) = \Phi(x) = \frac{1}{2\pi}\int_{\mathbb{R}} e^{-ixz} f(z)\, dz, \tag{3.3}$$

where each function f is integrable and defines a unique FT $\mathcal{F}[f]$.

It is possible to invert the FT and retrieve the function f

$$\mathcal{F}^{-1}[\mathcal{F}[f]](z) = f(z) = \frac{1}{2\pi}\int_{\mathbb{R}} e^{-ixz}\mathcal{F}[f](x)\, dx. \tag{3.4}$$

In the financial context, f will be a probability density function of a random variable, and actually, the FT is its characteristic function. The importance of the inverse of the FT is that given the characteristic function of any random variable, it is possible to obtain its density. This can be useful for random variables that do not have a close formula for the density; For instance, the LTS processes at time t when $\alpha \neq 0$ or $\alpha \neq 1/2$.

In [14], Theorem 3.2, it was developed a general formula for option valuation using the FT and it was also discussed the particular formula to price an European call option. The aforementioned formula is presented in the next proposition, where it is written in terms of forward prices.

Proposition 3.2: ***Option Pricing Formula [14]:*** *The formula to price an European Call option with strike price K, time to maturity T and forward price $F_0(T)$ is given by:*

$$C(K,T) = B_T F_0(T)\left[1 - e^{-x/2}\int_{-\infty}^{\infty}\frac{dz}{2\pi}\, e^{-izx}\phi^c\left(-z-\frac{i}{2}\right)\frac{1}{z^2+\frac{1}{4}}\right], \tag{3.5}$$

where B_T is the discount factor, $\phi^c(u)$ is the characteristic function of f_T and $x = -log(K/F_0(T))$[1]

To use this formula, it is necessary to use numerical methods to calculate the integral, which can be approximated by the next sum

$$\int_{-\infty}^{\infty} e^{-izx} g(z)\, dz \approx \sum_{j=0}^{N-1} e^{-iz_j x} g(z_j) dz, \tag{3.6}$$

where $g(z) = \frac{1}{2\pi}\phi^c\left(-z-\frac{i}{2}\right)\frac{1}{z^2+\frac{1}{4}}$ and the points z_j are chosen to be equidistant and with an spacing small enough over a sufficiently large interval to obtain a good approximation. It is important to note that this expression is useful for a particular point x, which value depends particularly on the strike value K. There exist the possibility to calculate N sums, each one with a different strike, at the same time and obtain N prices by using the FFT.

[1] Variable x is known as the moneyness of the option.

2.2 Fast Fourier Transform

The FFT is a numerical algorithm, which is for example described in [15], that simultaneously computes N sums of the form

$$FFT(f_k^*) = \sum_{j=1}^{N} e^{-i\frac{2\pi}{N}(j-1)(k-1)} f_j, \qquad \forall k = 1, ..., N \tag{3.7}$$

During the calibration process, this valuation method is particularly useful because it allows to valuate all the options for an specific maturity at the same time with a better computational performance than when it is computed each option separately. The number of operations needed for the FFT method is of order $o(N\log(N)$ while the order when pricing the options separately is $o(N^2)$.

To express Equation (3.6) in a way where it is possible to use the FFT, it is necessary to define the two partitions over the moneyness (x_j) and over the domain of the characteristic function (z_k)

$$\begin{cases} z_j = z_1 + (j-1)dz & j = 1, ..., N \\ x_k = x_1 + (k-1)dx & k = 1, ..., N, \end{cases} \tag{3.8}$$

where it needs to be fulfilled the condition $dxdz = \frac{2\pi}{N}$. Substituting definitions of z_k and x_j into Equation (3.6) leads to

$$\begin{aligned}
\sum_{j=1}^{N} e^{-iz_j x_k} g(z_j)dz = & \sum_{j=1}^{N} e^{-i(z_1+(j-1)dz)(x_1+(k-1)dx)} g(z_j)dz \\
= & \sum_{j=1}^{N} e^{-i[z_1x_1+z_1(k-1)dx+(j-1)dzx_1+(j-1)dz(k-1)dx]} g(z_j)dz \\
= & \sum_{j=1}^{N} e^{-i[z_1(x_1+(k-1)dx)+(j-1)dzx_1+\frac{2\pi}{N}(j-1)(k-1)]} g(z_j)dz \\
= & dze^{-iz_1x_k} \sum_{j=1}^{N} e^{-i\frac{2\pi}{N}(j-1)(k-1)} e^{-i(j-1)dzx_1} g(z_j) \\
= & dze^{-iz_1x_k} FFT(f_k^*),
\end{aligned}$$

where in this particular case $f_j = e^{-i(j-1)dzx_1} g(z_j)$. The output will be a vector with N values, where each value is the approximation of the integral for the corresponding moneyness x_j. To obtain the call price for the moneyness x_j, it is just needed to substitute the value of the integral in Equation (3.5).

3 Model Calibration

Calibration is a mathematical procedure which involve adjusting the model parameters of a particular model to match observed market prices. Therefore, the theoretical model studied in Section 1 of this chapter will be calibrated on a set of call options traded in the market. The result of the calibration for a given date, will be the parameters $\bar{\eta}, \bar{\kappa}$ and $\bar{\sigma}$, which can be used to re-price the market options, devise hedging strategies, or valuate exotic derivatives over the same underlying.

3.1 How to Calibrate

To calibrate any financial model, the aim is to find the parameters that better fit the market data. Following [16], such parameters can be obtained by minimizing different objective functions. An example of an objective function that considers market and model prices is

$$\min_p \frac{1}{N} \sum_{n=1}^{N} (C_n^* - C_n^{mod}(p))^2, \tag{3.9}$$

where C_n^* corresponds to the market price of the n call option and $C_n^{mod}(p)$ is the call price using the pricing model with the parameter vector p. It is possible to use another objective function that takes into account the relative differences in prices

$$\min_p \frac{1}{N} \sum_{n=1}^{N} \left(\frac{C_n^* - C_n^{mod}(p)}{C_n^*} \right)^2. \tag{3.10}$$

There are other objective functions that compare the implied volatility, such as

$$\min_p \frac{1}{N} \sum_{n=1}^{N} (\sigma_n^* - \sigma_n^{mod}(p))^2, \tag{3.11}$$

and

$$\min_p \frac{1}{N} \sum_{n=1}^{N} \left((\sigma_n^* - \sigma_n^{mod}(p)) \frac{\partial C_n^{BSM}}{\partial \sigma_n^*} \right)^2, \tag{3.12}$$

where σ^* is again the market implied volatility and σ^{mod} is the BSM implied volatility using the price of the option obtained with the pricing model that is being calibrated.

It can be observed that all the previous functions involve the mean square of certain differences. This is called the mean squared error (MSE). Therefore, the goal in the calibration process is to find the parameters of the model, represented by the vector p, that give the minimum possible MSE.

3.2 Optimization Method

To minimize the chosen objective function, the Nelder-Mead simplex method will be used, which is a brute force algorithm to find parameters that retrieves the minimum error. This method is often used to minimize functions which gradient is difficult or impossible to compute, which means that the derivatives are not needed during the optimization process. However, one drawback of this method is that the algorithm can be sensitive to the choice of parameters, such as the size of the initial simplex and the termination criteria; Additionally, the algorithm can be slow to converge for some types of functions depending in the tolerance that is set to accept one point as minima.

Chapter 4

Analysis and Results

1 Data Description

The option data used in this thesis consists of a dataset containing observations of daily option prices of European call options with one underlying: EURO STOXX 50 index in three different time windows, details and motivation to analyze this information are given in the next subsections.

1.1 Time Spans

The dataset covers three different time periods:

- The first period is from January 2017 to December 2017.
- The second period is from November 2019 to November 2020.
- The third is from March 31^{st} to April 28^{th}, 2023.

With the study of these time windows, the idea is to analyze the levels and the development of the calibrated parameters of the ATS model under different market conditions. The first time window was characterized by different political events that had a significant repercussion in the global economy, some of the main events during this year were:

- The uncertainty over political events that happened in the second semester of 2016 such as Brexit, the election of President Donald Trump in the United States, and tensions on the Korean peninsula continued to affect the global economy by increasing the volatility in financial markets.
- The US Federal Reserve and other central banks began to tighten monetary policy, raising interest rates and reducing their asset purchases.
- Trade tensions between the US and China began to escalate in 2017, with both countries imposing tariffs on each other's goods. This created uncertainty for businesses and consumers and had implications for global trade and economic growth.

During the window of 2020, some of the main events that triggered a global recession and that affected the global economy were

- The pandemic cause by the COVID-19, which began in late 2019 but spread rapidly in 2020, leading to lockdowns, travel restrictions, and disruptions to global supply chains. The pandemic caused a sharp contraction in the global economy.
- Due to the pandemic, several governments and central banks responded with massive fiscal and monetary stimulus measures, including direct cash payments to households, loans to businesses, and asset purchases.

- Because of the travel restrictions and lockdowns, it was observed sharp decline in oil prices, which had significant implications for oil-exporting countries and the global energy industry.
- The trade tensions between the US and China continued in 2020 and in combination with the pandemic, disruptions in global trade and supply chains were exacerbated.

The last small window of April 2023 seeks to portrait the calibration results over the most recent option prices by the time this thesis is written. According to the world economic outlook realized by the International Monetary Fund, the main drivers of the global economy for April, 2023 [17], are

- The observed high level of inflation combined with the monetary and fiscal policies followed by the central banks.
- The ongoing effects of the conflict between Russia and Ukraine.

1.2 Underlying Asset

The EURO STOXX 50 index (SX5E) was chosen because it is one of the main indexes of the Eurozone which represent the overall performance of the equity market in this region. The previous implies that the option over this index are one of the most liquid in the equity market worldwide, which makes this index suitable for benchmark purposes.

The SX5E index is constructed with 50 of the largest and most liquid companies in the Eurozone including companies from various sectors, such as financial services, energy, and consumer goods. The index is weighted by market capitalization, meaning that larger companies have a greater impact on the index's overall performance; However, it contains a cap of 10% to prevent that a company will dominate the index.

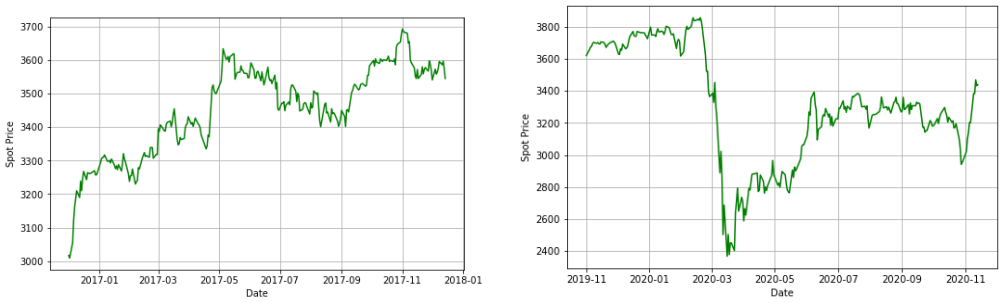

Figure 4.1: EURO STOXX 50 index during different time spans.

2 Data Processing

There were two sources for the European call option datasets that were used for the calibration. The datasets corresponding to the first two time spans, i.e., information from years 2017 and 2020, were obtained from the data product IvyDB Europe provided by OptionMetrics [18]. On the other hand, the information of the third time span was obtained directly from the EUREX webpage [19].

The information from IvyDB Europe consist of daily implied volatility surfaces considering call options traded in Eurex. It is important to mention that the volatility surfaces are already processed and interpolated by the provider and the call option prices were retrieved from the implied volatilities. The next bullets summarize the main aspects in the information and methodology followed by IvyDB Europe

- During the two time spans, there are a total of 529 days/volatility surfaces.
- In each day, there are considered 10 maturities ranging from 30 to 730 calendar days, and for each maturity there were calculated 13 implied strike prices.
- The interest rate that were used during the calculations corresponds to the zero-coupon rate that has a maturity equal to the option's expiration, and that is obtained by linearly interpolating between the two closest zero-coupon rates on the zero curve. Such curves were also provided by IvyDB Europe.
- The dividend yield for the index is calculated based on linearized put-call parity. Where the present value of the dividend payments is:

$$PV(div) = Put - Call + (S_0 - K) + K(e^{rT} - 1), \tag{4.1}$$

  where PV refers to the present value, r is the interest rate to the option expiration and T is time to maturity in years. Then, the implied dividend yield is: $q = \frac{PV(div)}{S_0 \times T}$.
- The price of each option was retrieved from the implied volatility and by using the appropriate interest and dividend rate.

For the time span corresponding to April, 2023, call and put option prices were obtained from [19] by using web scrapping techniques. The data considered for the calibration is explained as follows

- For each day, the options which maturity was over the next nine months (May 23-January 24) were considered for the analysis. It is a standard that the options expires in the third Friday of the corresponding month, so the maturity days were calculated accordingly. Additionally, the data set is composed by the settlement price, and no smoothing or interpolation was done.
- For each maturity, a total of 13 option prices were used. The way these options were chosen is explained as follows: First, the closest strike to the ATM option was identified, then the six strikes over and under this ATM value were taken. The previous gave us a total of six options OTM, six option ITM and one option ATM, which is a total of 13 options.
- To calculate the Forward price, the put-call parity was used over the ATM option and the zero-coupon EURIBOR rate. The Forward price was calculated by

$$F_0(T) = (Call^{ATM} - Put^{ATM})e^{rT} + K, \tag{4.2}$$

  where $Call^{ATM}$ and Put^{ATM} are the corresponding call and put at the money prices, r is the zero-coupon EURIBOR rate and K is the strike.

  It is important to highlight that by obtaining the forward price in this way, the implicit dividend yield is included in the price, so no projections or additional calculations needs to be performed.
- The volatility surfaces of the period were calculated by inferring the implied volatility from the Black-Scholes formula for each of the option prices. Since there is no close formula to obtain the implied volatility, the Newton-Raphson method was used.

3 Calibration Procedure

In [5], the calibration was performed by minimizing the Euclidean distance between model and market prices, which means that the squared root of Equation 3.9 was used. A rough description of the process to calibrate the volatility surface in [5] is as follows: For each maturity that was traded in the market, it was calibrated a LTS process, so the total number of parameters retrieved was three multiplied by the number of maturities. Subsequently, an analysis of the parameters η_t and κ_t was conducted where it was shown that they follow the power-law scaling properties discussed in Section 5.2 and the values of β and δ were found to have a value of 1 and 1/2, respectively. The consistency of the value of these two parameters with empirical equity market characteristics was later proven in [12].

For this thesis, Equation (3.9) will be considered, but instead of calibrating each maturity separately, the parameters β and δ will be fixed to 1 and 1/2, respectively, following [12]. Finally, the minimization of the chosen objective function will be performed using all the available maturities and the parameters $\bar{\eta}, \bar{\kappa}$ and $\bar{\sigma}$, as well as the MSE, will be retrieved.

As mentioned in the introduction, the idea is to compare the level of the parameters and the MSE between the LTS and ATS processes when they consider two different subordinators: the VG and the NIG process. In total, for each analyzed day, the next four processes will be compared:

1. ATS process with the VG process as subordinator (ATS-VG)
2. LTS process with the VG process as subordinator (LTS-VG)
3. ATS process with the NIG process as subordinator (ATS-NIG)
4. LTS process with the NIG process as subordinator (LTS-NIG)

4 Results

This section will show the experimental results of the calibration process and will mention the main insights after analyzing each of the time periods.

4.1 First Period: December 2016 - December 2020

After the presidential elections held in the United States in November 2016, the economic environment experienced an increment in the volatility levels that remained throughout 2017. Figure 4.2 shows the volatility surfaces for three arbitrary dates during December 2016, May 2020 and November 2020. It is possible to observe that the volatilities presented a steep slope in the short term maturities, this situation is of relevant importance in the calibration process since the parameter that is mainly affected is $\bar{\eta}$, which also affects the average volatility $\bar{\sigma}$, this situation will be shown during this and the subsequent subsections.

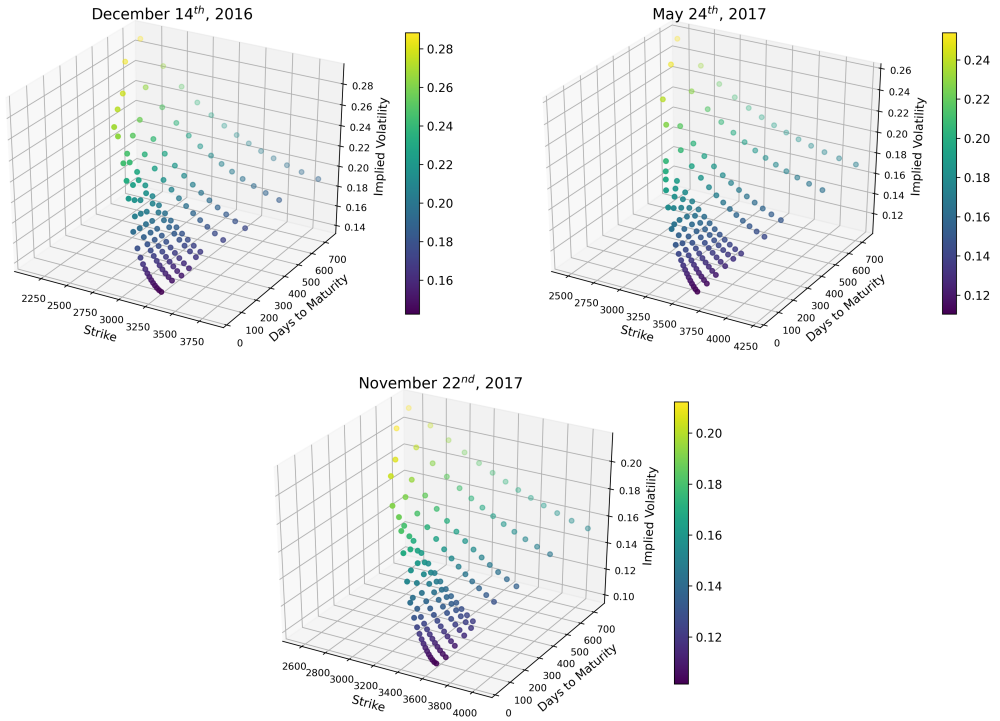

Figure 4.2: Market volatility surface as of dates: December 14^{th}, 2016, May 24^{th}, 2017 and November 22^{nd}, 2017.

Table 4.1 contains the results of the calibration for December 14^{th}, 2016. It is possible to observe that for all the models the average volatility is located around the 19%. Both, the ATS and the LTS processes present a better approximation to the market implied volatility when the subordinator is the NIG process than when the subordinator is the VG process; However, it is noticeable the improvement in the calibration between the ATS and LTS models when comparing the MSE.

Model	$\bar{\eta}$	$\bar{\kappa}$	$\bar{\sigma}$	**MSE**
ATS-VG	4.663	0.809	0.194	4.517
LTS-VG	3.997	0.719	0.195	53.956
ATS-NIG	5.506	1.081	0.188	0.958
LTS-NIG	4.494	0.968	0.190	23.787

Table 4.1: Calibrated parameters of the ATS and LTS processes. Date: December, 14^{th}, 2016.

During 2020, the average volatility in the market slightly decreased, so the parameters presented a similar behavior as the one observed in December, 2016. Table 4.2 shows the calibration results for May 24^{th}, 2017, where again the subordinator that better fits the volatility surfaces is the NIG process in the ATS and LTS processes.

Model	$\bar{\eta}$	$\bar{\kappa}$	$\bar{\sigma}$	**MSE**
ATS-VG	6.032	0.803	0.161	5.271
LTS-VG	2.405	1.301	0.188	56.388
ATS-NIG	7.342	1.114	0.156	1.456
LTS-NIG	2.251	2.545	0.193	20.393

Table 4.2: Calibrated parameters of the ATS and LTS processes. Date: May, 24^{th}, 2017.

To observe how these models fit the volatility smiles, Figure 4.3 compares the market implied volatility with the smiles generated by the ATS and the LTS models, respectively. The fit of the ATS model is clear for all the maturities, and for the LTS model is notorious the difference for the smile with time of 20 days.

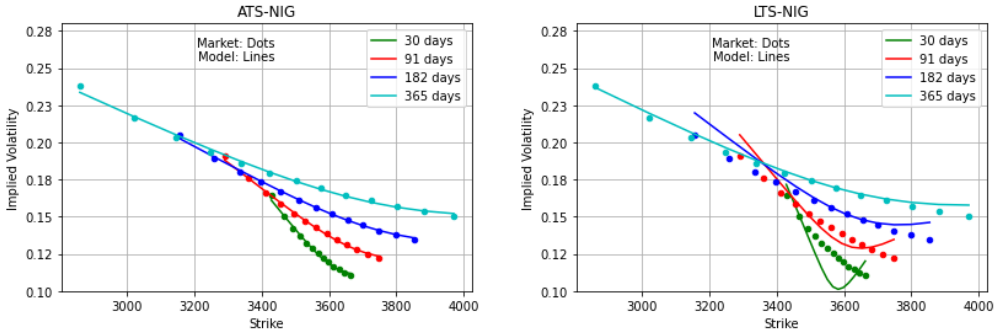

Figure 4.3: Comparison of implied volatilities between ATS, LTS processes with the NIG as subordinator and the market for multiple maturities. Data as of date: May, 24^{th}, 2017.

Finally, as the year continued, the volatility smiles showed a downward trend. In Table 4.3 are shown the calibrated parameters for November 22^{nd}, 2017. It is possible to see that the parameters of the ATS and LTS processes continued in similar levels as the previous dates but the MSE improved in both cases. It was consistent that the volatility smiles better fitted the market data when the NIG process was used as subordinator.

Model	$\bar{\eta}$	$\bar{\kappa}$	$\bar{\sigma}$	**MSE**
ATS-VG	6.579	0.646	0.142	0.744
LTS-VG	2.949	1.120	0.165	29.517
ATS-NIG	8.961	0.633	0.132	0.063
LTS-NIG	2.980	1.880	0.166	11.967

Table 4.3: Calibrated parameters of the ATS and LTS processes. Date: November, 22^{nd}, 2017.

4.2 Second Period: November 2019 - November 2020

As mentioned in the previous section, during 2020 was observed a significant increase in the volatility levels observed in the market due to the pandemic caused by the COVID-19. In Figure 4.4 are shown three volatility surfaces: the first one in November, 2019, the second one in March, 2020 and the last one in November, 2020. The volatility at the end of 2019 was around 14% for all the option maturities, while in March, 2020, the volatility levels raised to 60% in options that were deep in the money. At the end of 2020, the volatility decreased to levels near the 30%.

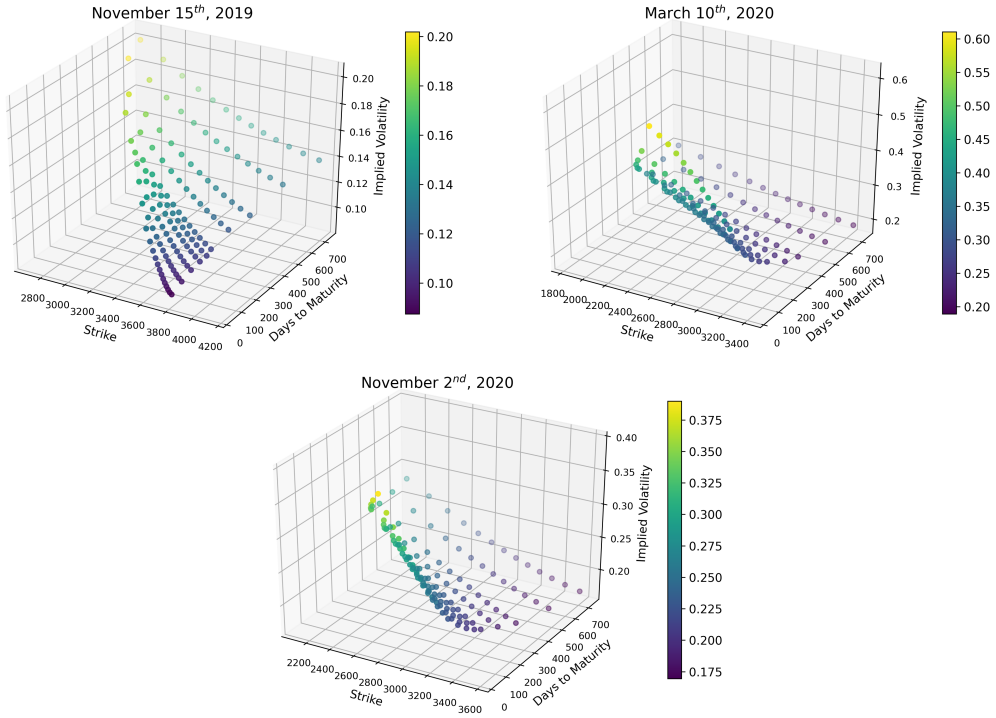

Figure 4.4: Market volatility surface as of dates: November 15^{th}, 2019, March 10^{th}, 2020 and November 2^{nd}, 2020.

The calibration for November 15^{th}, achieved relatively good results for both, the ATS and LTS models. In Table 4.4 are shown the parameters obtained from the calibration for the ATS and the LTS model using the processes VG and NIG as subordinators. It is possible to observe the good calibration results in the ATS cases.

Model	$\bar{\eta}$	$\bar{\kappa}$	$\bar{\sigma}$	**MSE**
ATS-VG	1.049	0.745	0.131	1.396
LTS-VG	3.602	1.087	0.149	26.081
ATS-NIG	0.848	0.888	0.135	0.159
LTS-NIG	3.812	1.707	0.148	7.249

Table 4.4: Calibrated parameters of the ATS and LTS processes. Date: November, 15^{th}, 2019.

During March, 2020, it was observed that the parameter $\bar{\eta}$ in the both model reacted drastically when the volatility smile got more and more steep. In March 2020, was reached an extreme case where the volatility smiles were concave in the short term. Table 4.5 show the calibrated result for March 24^{th}, were it was shown that with the implied volatility having this shape, the calibration failed in the LTS case. On the other hand, the important increase in the parameter $\bar{\eta}$ affected significantly the value of $\bar{\sigma}$, and it stopped reflecting the average volatility of the market due to the shape of the volatility surface.

Model	$\bar{\eta}$	$\bar{\kappa}$	$\bar{\sigma}$	**MSE**
ATS-VG	8.996	0.868	0.251	1.06536
LTS-VG	376.878	0.0916	0.049	2457.61
ATS-NIG	64.5911	1.978	0.143	1.15689
LTS-NIG	1082.46	0.042	0.036	2481.24

Table 4.5: Calibrated parameters of the ATS and LTS processes. Date: March, 10^{th}, 2020.

As for the third date, November 2^{nd}, the parameters showed a similar behaviour as in March 10^{th}. The parameter $\bar{\eta}$ continued being high particularly in the LTS model and the calibration failed. Table 4.6 show the results of the calibration for each of the analyzed models.

Model	$\bar{\eta}$	$\bar{\kappa}$	$\bar{\sigma}$	**MSE**
ATS-VG	3.847	1.050	0.243	0.00507
LTS-VG	277.497	0.150	0.047	806.364
ATS-NIG	6.25922	2.783	0.200	0.4753
LTS-NIG	549.062	0.0795	0.0395	812.159

Table 4.6: Calibrated parameters of the ATS and LTS processes. Date: November, 2^{nd}, 2020.

It is very important to remember that as explained in Section 2, the information from years 2017 and 2020 corresponds to market data that was already processed and interpolated, this situation may have affected the results for the calibration of each model studied in the present work since processed data may not entirely reflect the market conditions for the options analyzed in this thesis. To test and calibrate the models using raw market data, the next time period was proposed to bring this analysis.

4.3 Third Period: April 2023

In Figure 4.5 it is shown the log-MSE of the calibration process during April, 2023, for the VG and the NIG process for both, the LTS and ATS processes. It is possible to observe how it is significantly better the calibration for the ATS processes over the LTS processes and, in in this period, the ATS process using the NIG process as subordinator outperforms the corresponding ATS process using the VG process.

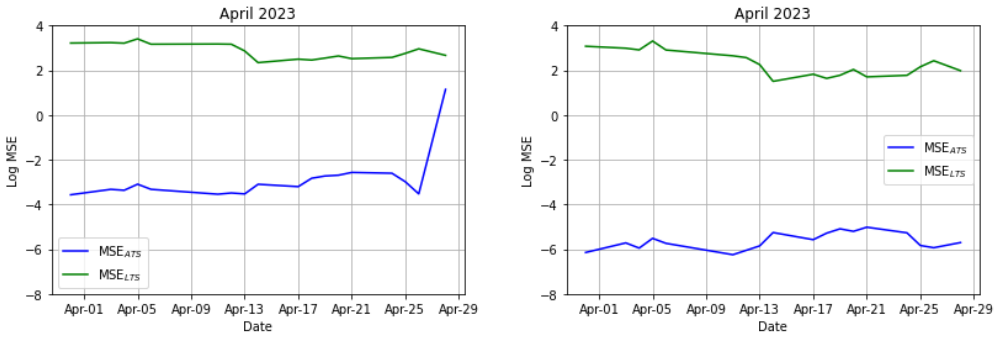

Figure 4.5: Log-MSE of the calibration of ATS and LTS models with the VG (left) and NIG (right) processes.

In Figures 4.6, 4.7 and 4.8 it is possible to observe the development of the parameters $\bar{\eta}, \bar{\kappa}$ and $\bar{\sigma}$, respectively, for the ATS and LTS processes using the two different subordinators. During the first days of the month it is remarkable the difference in the parameter $\bar{\eta}$ between the ATS and LTS processes, during the second half of the month the value of this parameter was around 9 for the LTS processes while for the ATS processes remains in a level of 1 for the full month.

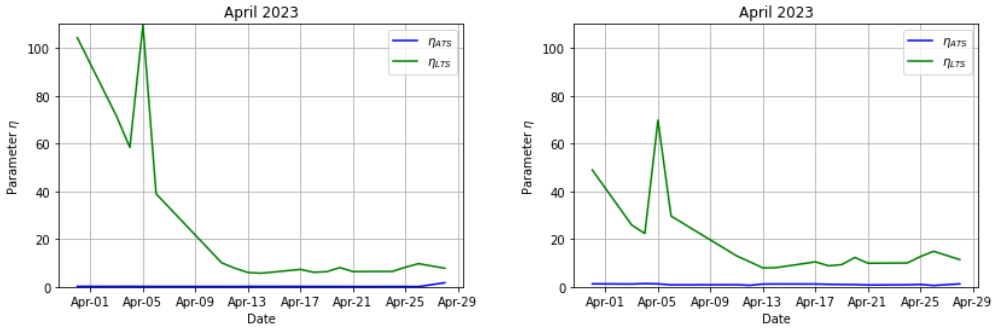

Figure 4.6: Development of the parameter η in the ATS and LTS models with the VG (left) and NIG (right) processes.

In case of the parameter $\bar{\kappa}$, it presented an stable behaviour for the four models for the whole month, with an exception in the last day in the LTS process with the VG process as subordinator.

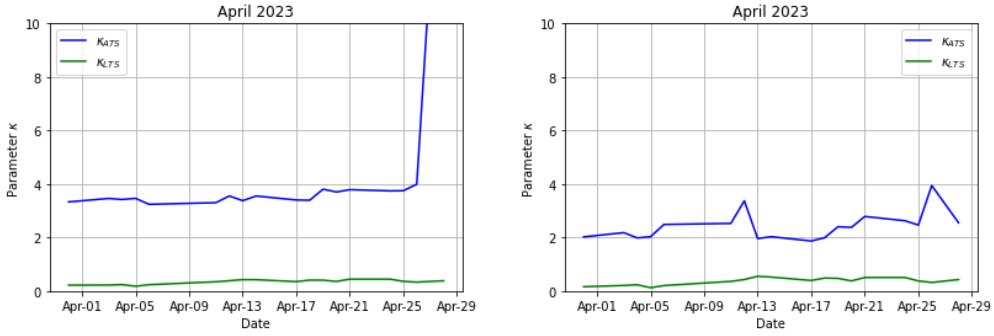

Figure 4.7: Development of the parameter κ in the ATS and LTS models with the VG (left) and NIG (right) processes.

Finally, the average volatility is shown in Figure 4.8 with the development of the parameter $\bar{\sigma}$. The first day of the month the volatility is low for both of the LTS processes, this is due to the high values of $\bar{\eta}$ that were observed during the same period. For the rest of the month, it is possible to observe that the average volatility is quite similar in all the cases, in general the average volatility in ATS process using the VG process is slightly higher that the ATS process using the NIG process.

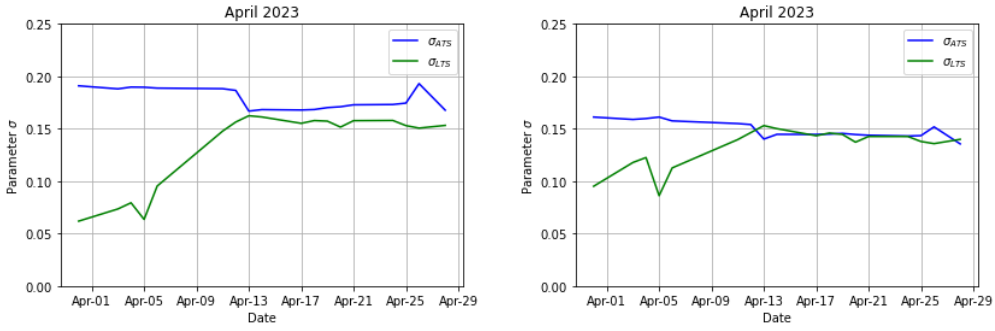

Figure 4.8: Development of the parameter σ in the ATS and LTS models with the VG (left) and NIG (right) processes.

To show the calibration results for an arbitrary date, it was chosen April 18^{th}, 2023. Since it was observed a great similarity in the results obtained with the VG and NIG processes, it will be shown the comparison between the ATS and LTS processes using the NIG process as subordinator.

The parameters obtained are presented in Table 4.7, where it is important to highlight the low mean squared error achieved by the ATS process.

Model	$\bar{\eta}$	$\bar{\kappa}$	$\bar{\sigma}$	**MSE**
ATS-NIG	1.049	1.992	0.145	0.00507
LTS-NIG	8.796	0.484	0.146	5.14581

Table 4.7: Calibrated parameters of the ATS and LTS processes with the NIG process as subordinator. Date: April, 18^{th}, 2023.

To illustrate how the models fit the implied volatility smile and the European call option prices, in Figure 4.9 are shown the results for three maturities: May 2023, September 2023 and January 2024. In general, the LTS model presented a good calibration compared to other models that can be observed in the market and that contain a higher number of parameters; However, it is clear the excellent results achieved by using the ATS processes, in this case with the NIG process as subordinator.

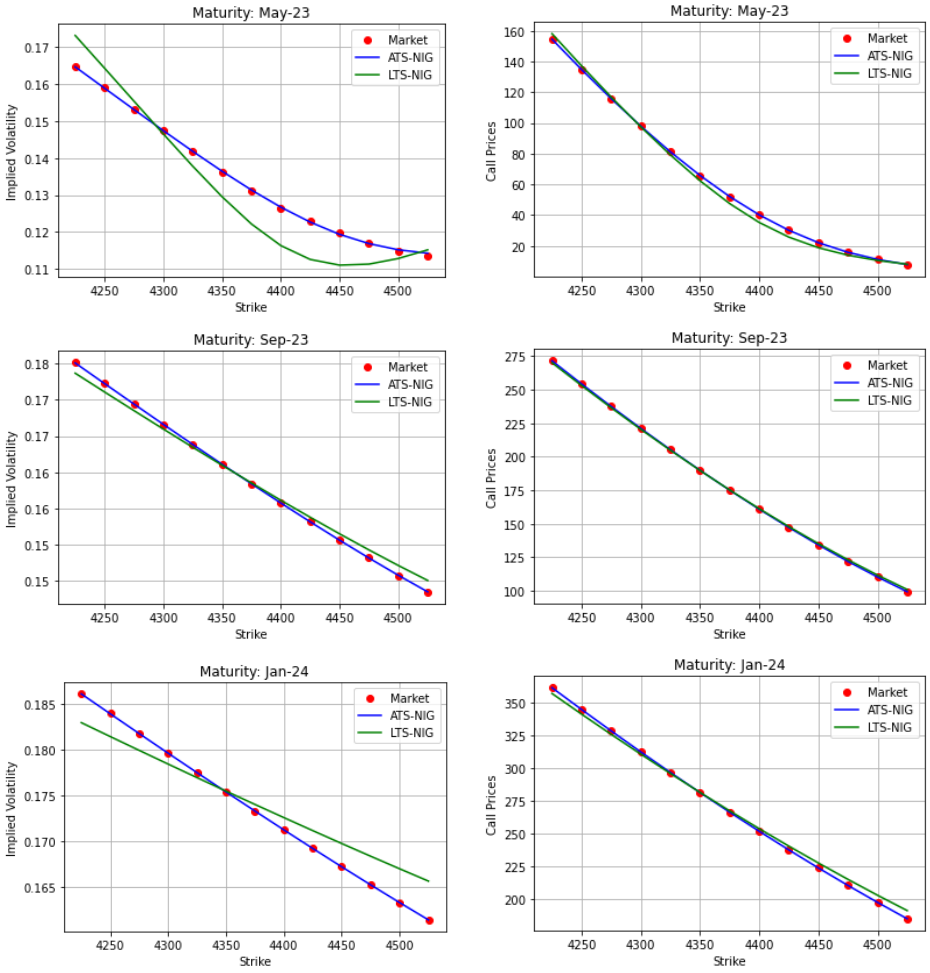

Figure 4.9: Comparison of implied volatilities and European Call prices between ATS, LTS processes with the NIG as subordinator and the market. Data as of date: April, 18^{th}, 2023.

Chapter 5

Conclusion

In this master thesis, the application of ATS processes in the calibration of the volatility surface of the EURO STOXX 50 over different time periods was investigated; In particular, the behavior of the parameters was studied and the calibration fitting to market data of the ATS processes was compared (using the MSE) with their corresponding LTS processes when using two different subordinators: the VG and the NIG process.

The experimental results showed that the ATS processes outperform the LTS processes, independent of the associated subordinator, in every of the three analyzed time spans. During the years 2017 and 2020, it was observed that when the volatilities present a steep slope in the short term maturities, the parameter that is mainly affected is $\bar{\eta}$, which may generate a reduction in the average volatility $\bar{\sigma}$. For April, 2023, the analysis was made over raw market data and the calibrated model reproduced the market volatility surface almost exactly.

Future work and discussion

Firstly, it would be beneficial to explore additional time spans and economic events to gain a more comprehensive understanding of the parameter stability in LTS processes. Additionally, investigating the impact of different calibration techniques and optimization methods on the model's performance and parameter stability could provide valuable insights. Furthermore, extending the analysis to other market indices or individual stocks would allow for a broader assessment of the model's applicability.

Bibliography

[1] D. B. Madan and E. Seneta, 'The variance gamma (VG) model for share market returns,' *Journal of Business*, vol. 63, no. 4, pp. 511–524, 1990.

[2] D. B. Madan *et al.*, 'The variance gamma process and option pricing,' *Review of Finance*, vol. 2, no. 1, pp. 79–105, 1998.

[3] Barndorff-Nielsen, 'Normal inverse gaussian distributions and stochastic volatility modelling,' *Scandinavian journal of statistics*, vol. 24, no. 1, pp. 1–13, 1997.

[4] R. Cont and P. Tankov, *Financial Modelling with Jump Processes*. Chapman and Hall/CRC, 2003.

[5] M. Azzone and R. Baviera, 'Additive normal tempered stable processes for equity derivatives and power law scaling,' *Quantitative Finance*, Published Online, 2021.

[6] K. I. Sato, *Lévy Processes and Infinitely Divisible Distributions*. Cambridge: Cambridge University Press, 1999.

[7] F. Benth and C. Sgarra, 'The risk premium and the esscher transform in power markets,' *Stochastic Analysis and Applications*, vol. 30, no. 1, pp. 20–43, 2012.

[8] P. Carr *et al.*, 'Self-decomposability and option pricing,' *Mathematical Finance*, vol. 17, no. 1, pp. 31–57, 2007.

[9] J. P. Nolan, *Univariate Stable Distributions: Models for Heavy Tailed Data*. Springer Cham, 2020.

[10] R. C. Merton, 'Option pricing when underlying stock returns are discontinuous,' *Journal of Financial Economics*, vol. 3, no. 1-2, pp. 125–144, 1976. [Online]. Available: https://doi.org/10.1016/0304-405X(76)90022-2.

[11] Barndorff-Nielsen, 'Processes of normal inverse gaussian type,' *Finance and Stochastics*, vol. 2, no. 1, pp. 41–68, 1998.

[12] M. Azzone and R. Baviera, 'Short-time implied volatility of additive normal tempered stable processes,' *Quantitative Finance*, Published Online, 2021.

[13] R. Baviera, 'Gigi model: A simple stochastic volatility approach for multifactor interest rates,' 2007. [Online]. Available: https://papers.ssrn.com/sol3/papers.cfm?abstract_id=977479.

[14] A. L. Lewis, 'A simple option formula for general jump-diffusion and other exponential lévy processes,' 2001.

[15] K. Chourdakis, *Financial Engineering, A brief introduction using the Matlab systems*. 2008.

[16] Y. Hilpisch, *Derivatives Analytics with Python: Data Analysis, Models, Simulation, Calibration and Hedging*. (Wiley finance series). 2015.

[17] IMF, *World economic outlook, april*, Accessed: 2023-04-27, 2023. [Online]. Available: https://www.imf.org/en/Publications/WEO/Issues/2023/04/11/world-economic-outlook-april-2023.

[18] O. LLC, *Data products option metrics description.* Accessed: 2023-04-27. [Online]. Available: https://optionmetrics.com/data-products/.

[19] EUREX, Accessed: 2023-04-27. [Online]. Available: https://www.eurex.com/ex-en/.